



#### **OPEN ACCESS**

EDITED BY

Rebecca Mott, WSL Institute for Snow and Avalanche Research SLF, Switzerland

REVIEWED BY

Shaohua Lei,

Nanjing Hydraulic Research Institute, China Tina Sona.

Jiangsu Wuxi Environmental Monitoring

Center, China

Ningjun Wang,

Panzhihua University, China

#### \*CORRESPONDENCE

Xiaoyue Zeng,

RECEIVED 19 June 2025 ACCEPTED 22 August 2025 PUBLISHED 24 October 2025

Zhang J, Zeng X, Wan J, Liu J and Xia Z (2025) Advances and prospects in reconstruction approaches for snow cover mapping using polar-orbiting satellites. Front. Earth Sci. 13:1649808. doi: 10.3389/feart.2025.1649808

© 2025 Zhang, Zeng, Wan, Liu and Xia. This is an open-access article distributed under the terms of the Creative Commons Attribution License (CC BY). The use, distribution or reproduction in other forums is permitted, provided the original author(s) and the copyright owner(s) are credited and that the original publication in this journal is cited, in accordance with accepted academic practice. No use, distribution or reproduction is permitted which does not comply with these terms.

## Advances and prospects in reconstruction approaches for snow cover mapping using polar-orbiting satellites

Jun Zhang<sup>1</sup>, Xiaoyue Zeng<sup>2,3,4</sup>\*, Jun Wan<sup>2,3,4</sup>, Jinghui Liu<sup>2,3,4</sup> and Zhihong Xia<sup>2,3,4</sup>

<sup>1</sup>China Yangtze Power Co., Ltd., Yichang, China, <sup>2</sup>Hubei Climate Center, Wuhan, China, <sup>3</sup>Three Gorges National Climatological Observatory, Yichang, China, 4Key Laboratory of Basin Heavy Rainfall, CMA, Wuhan, China

Snow cover is recognized as one of the most variable land cover parameters and plays a critical role in the global energy balance, climate change, and hydrological processes. Polar-orbiting satellites serve as the primary data source for monitoring both polar and global snow cover, providing wide coverage and high spatial resolution products. However, the utility of these snow cover products is significantly limited by data gaps caused by unfavorable observation conditions, such as cloud cover. Various reconstruction approaches are required to fill these gaps, depending on the snow cover product type (binary snow cover (BSC), normalized difference snow index (NDSI), or fractional snow cover (FSC)), snow characteristics, and availability of auxiliary datasets. This paper categorizes current reconstruction approaches into eight types: temporal filters, spatial filters, multisensor fusion, and the hidden Markov random field (HMRF) model for BSC mapping, as well as temporal and spatial interpolation methods, spatiotemporal reconstruction algorithms, machine learning-based reconstruction techniques, and data assimilation methods for NDSI or FSC mapping. This paper provides a comprehensive review of the principles, advantages, and limitations of these approaches and offers recommendations for their appropriate application. The discussion highlights that future improvements in snow cover reconstruction can be achieved through three key approaches. First, enhancing snow cover recognition algorithms will increase the accuracy of the original snow cover products, providing more reliable prior information for reconstruction. Second, careful consideration of spatiotemporal environmental factors, such as terrain, temperature, precipitation, solar radiation, and forest cover, along with the development of corresponding multisource data processing and fusion techniques, is essential. Third, further exploration of the synergy between machine learning and data assimilation could leverage their strengths in multisource data processing scenarios, offering novel insights for conducting snow monitoring and forecasting in complex environments. This review contributes to snow cover mapping and related research by offering a comprehensive analysis and guidelines for generating gap-filled snow cover products across a variety of spatiotemporal scales.

KEYWORDS

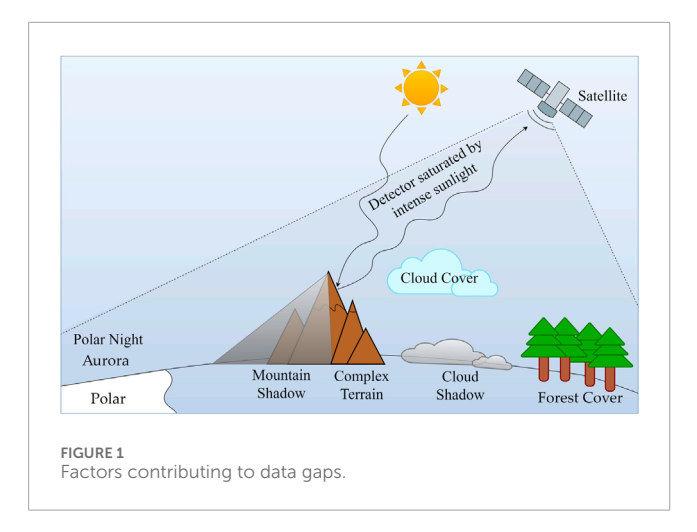
snow cover reconstruction, remote sensing, spatiotemporal methods, machine learning, data assimilation

### 1 Introduction

Snow cover is among the most dynamic natural components of the cryosphere and is crucial for the global energy balance, climate change, and the hydrological cycle (Tang et al., 2013; Li et al., 2018; Thackeray et al., 2019; Li et al., 2022). Snow cover enhances the surface albedo, reduces the absorption of solar shortwave radiation, and regulates the heat exchange process between the ground and the atmosphere. Moreover, it influences atmospheric circulation, serves as a key indicator for predicting regional precipitation, and plays a crucial feedback role in climate change (Dozier and Warren, 1982; Warren, 1982; Zhang, 2005; Warren, 2019; You et al., 2020). Additionally, snowmelt supplies water to more than one-sixth of the global population, affecting both the quality and quantity of downstream river water and serving as a vital source of river runoff (Armstrong et al., 2019; Han P. et al., 2019; Qin et al., 2020; Musselman et al., 2021; Yang et al., 2022). Consequently, as global warming alters the snow accumulation and snowmelt processes, the importance of snow cover monitoring becomes increasingly evident. Such monitoring procedures not only provide a critical foundation for scientific research, including snowmelt runoff forecasting and climate change assessment, but also offer essential support for disaster prevention, resource management, and water supply planning.

Currently, snow cover products derived from polar-orbiting satellites serve as crucial data sources for global snow cover monitoring and mapping, particularly in polar and high-latitude regions (Romanov et al., 2000; Dietz et al., 2012; Dixit et al., 2019; Zhang et al., 2023). These products typically utilize optical remote sensing data, which are more accurate than microwave products in identifying snow cover areas (SCAs) under clearsky conditions, particularly in regions with shallow snow cover (Wang et al., 2008; Foster et al., 2011; Dietz et al., 2012). These optical products offer advantages such as near-global coverage, wide availability, high precision, high temporal resolution (ranging from daily to several days), and spatial resolution from 5 km to several meters (Dixit et al., 2019; Muhuri et al., 2021; Zhang et al., 2023). Snow cover products derived from optical remote sensing are categorized into binary snow cover (BSC) products, normalized difference snow index (NDSI) products and fractional snow cover (FSC) products. BSC mapping is the traditional method used during the early stages of snow cover monitoring and involves simply classifying a pixel as either a snow or non-snow pixel, making it suitable for large-scale snow monitoring (Dobreva and Klein, 2011; Riggs and Hall, 2010; Rittger et al., 2013; Gafurov et al., 2016). With the development of remote sensing technology and algorithms, NDSI and FSC products, which provide continuous snow cover parameters, are becoming increasingly important in cryosphere and hydrology research. Specifically, the NDSI, which is the normalized difference between the green and shortwave infrared spectral bands, effectively distinguishes snow from clouds and other land features and can be used to generate both BSC and FSC products (Kulkarni et al., 2002; Salomonson and Appel, 2004; Mishra et al., 2016; Riggs et al., 2017; Li X. et al., 2019). FSC provides a more precise estimate of the areal extent of snow cover by estimating the fraction of a snow-covered pixel, which directly reflects the snow conditions of mixed pixels in complex terrain (Dozier et al., 2008; Dobreva and Klein, 2011; Tang et al., 2013; Haseeb Azizi et al., 2024; Xiao et al., 2024; Huang et al., 2025).

In practical applications, the above snow cover products inevitably suffer from data gaps due to a variety of influencing factors (Figure 1); however, reconstruction methods can address this issue, thereby enhancing the quality and utility of snow cover products. Cloud cover represents the primary cause of data gaps in snow cover products. The global mean cloud cover level, which is derived from MODIS products, is approximately 66% (Mao et al., 2019). The cloud cover levels in key ice and snow regions, including the North and South Poles, range from 50% to 80% (Kato et al., 2006), and the degree of cloud cover can reach 70% during the snowmelt season in alpine regions (Da Ronco and De Michele, 2014), which significantly impacts the availability and long-term comparability of snow cover products. The impact of cloud cover is a global, persistent, and non-negligible issue, making it the primary concern addressed by most current reconstruction methods. Cloud-induced shadows further exacerbate data gaps, particularly in high-resolution snow cover monitoring applications. In addition, accurate observation of snow cover beneath canopies is challenging at the surface in forested areas (Yang et al., 2023). Snow cover in mountainous areas with complex terrain is affected by satellite observation angles and mountain shadows, which lead to observation blind spots (Zhang et al., 2023). Although the effects of forest cover and complex terrain are relatively localized, they significantly increase the uncertainty of snow cover monitoring in mountainous and forested areas, posing major challenges for accurate reconstruction at the local scale. Additionally, adverse lighting conditions may also degrade the quality of snow cover products. Intense sunlight reflected from snow cover can saturate the utilized sensor (Zhang Y. et al., 2020). At the North and South Poles, the prolonged periods of darkness caused by the polar night render traditional optical remote sensing ineffective for observation tasks. Although nighttime light remote sensing offers new opportunities for polar snow cover monitoring, clouds and auroras may still obscure the acquired data (Huang et al., 2022a; Liu et al., 2023). These unfavorable factors may occur simultaneously depending on geographic and observational conditions, leading to increased data gaps and further reduced reliability of snow cover products. To mitigate the effects of these factors on snow cover products and reconstruct missing data, researchers have developed a variety of snow cover reconstruction methods (Gao et al., 2010a; Gao et al., 2010b; Richiardi et al., 2023). First, snow cover reconstruction enhances the continuity and timeliness of snow cover monitoring. Reconstructing historical snow cover datasets addresses issues such as the limited availability of remote sensing data and the insufficient number of observations acquired at remote mountain sites, analyzing snow cover characteristics across broad geographical areas over several decades, and providing long-term historical data for the operation and calibration of hydrological models (Gafurov et al., 2015). Second, the reconstructed snow cover products serve as crucial input data for estimating snow depth (SD), snow water equivalent (SWE) and other snow parameters, thereby reducing uncertainty in parameter retrieval. For example, recent snow depth products derived from Sentinel-1 SAR data utilize a gapless, daily binary snow cover product to indicate snow presence and minimize the influence of non-snow factors (Lievens et al., 2022; Hoppinen et al., 2024; Ying et al., 2025). The reconstructed snow



cover results can also be used as a mask to constrain the target snow cover area and assist in downscaling SD and SWE products to higher spatial resolutions, which is important for evaluating regional snow resources, analyzing the spatial distribution of snow cover with its generation and dissipation processes, and predicting future snowmelt runoff (Molotch and Margulis, 2008; Hall et al., 2010; Rittger et al., 2016).

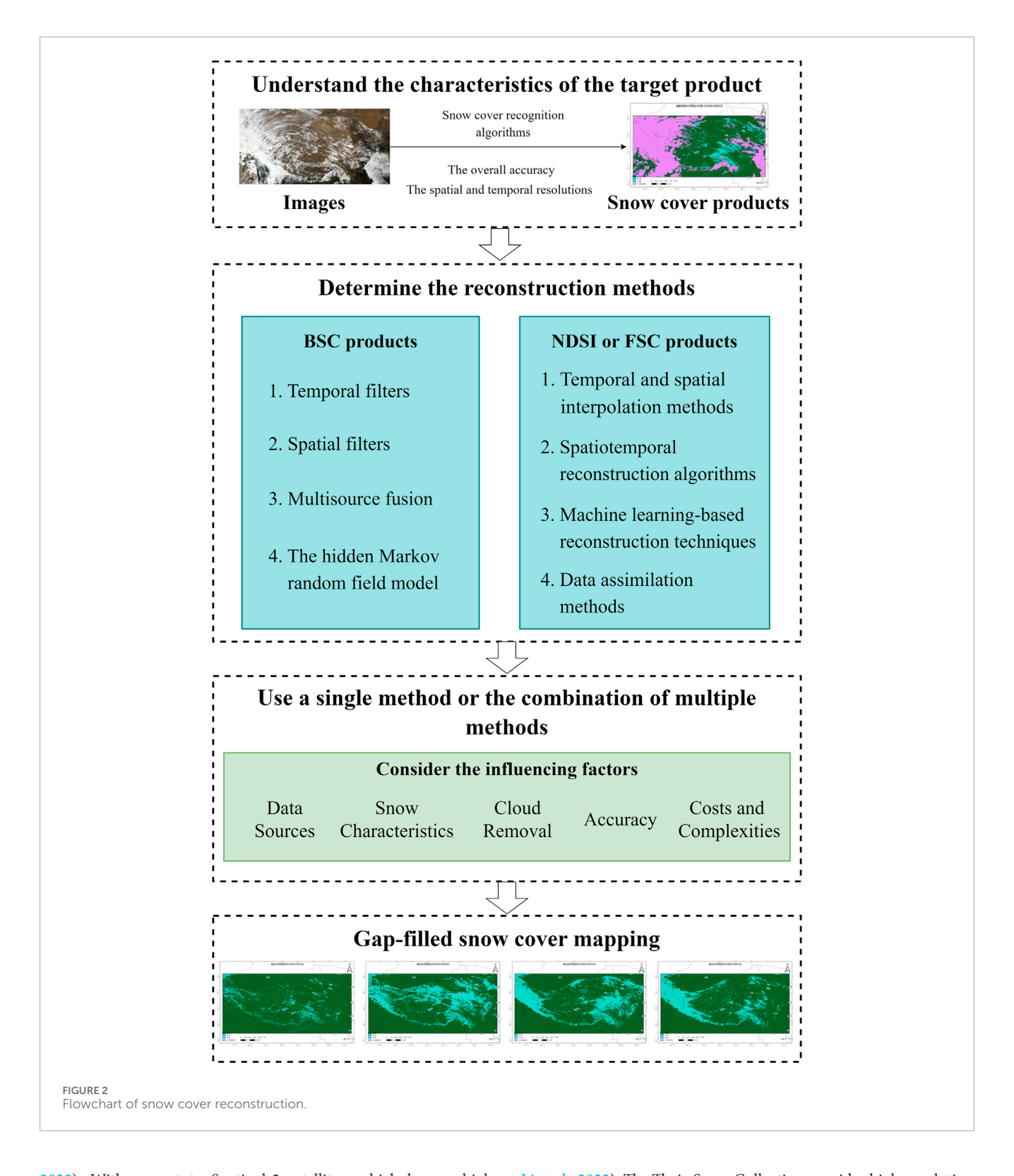
To this end, we provide a review of various reconstruction methods for snow cover products from polar-orbiting satellites and organize the paper according to the flowchart in Figure 2. Although previous research has discussed related methods for MODIS BSC products (Coll and Li, 2018; Li X. et al., 2019; Gao Y. et al., 2024), we broaden the scope of our exploration and address the following key points that have not been covered in prior studies.

- First, we briefly introduce the six primary data sources for monitoring snow cover from polar-orbiting satellites. We discuss their basic accuracies and characteristics to establish a foundation for subsequent research.
- 2. We focus on a comprehensive analysis of four reconstruction methods for NDSI or FSC mapping while providing a brief overview of the reconstruction methods for BSC mapping. Specifically, we offer recommendations for the appropriate application of each method. These insights can assist researchers in selecting suitable methods or refining existing approaches.
- By comparing current reconstruction methods, we highlight challenges within the existing research and propose future research directions, offering guidelines for generating gapfilled snow cover products for related scientific studies.

# 2 Snow cover products derived from polar-orbiting satellites

Before snow cover is reconstructed, understanding the characteristics of different snow cover products, including their original accuracy and resolution, is essential for selecting appropriate reconstruction methods.

Various types of snow cover products are derived from polarorbiting satellites (Table 1). Most official products still contain significant numbers of cloud or missing pixels (hereafter referred to as cloud pixels), with a few gap-filled exceptions (such as MOD10A1F and MYD10A1F). Snow cover products provide accurate clear-sky observations that serve as reliable prior data, forming the foundation for performing snow cover reconstruction. The most widely used snow cover products come from the Moderate Resolution Imaging Spectroradiometer (MODIS) onboard the Terra and Aqua satellites (Hall et al., 2010; Hall et al., 2019). The MODIS products are characterized by easy accessibility, wide coverage, and excellent snow monitoring capabilities, with overall accuracies typically exceeding 85% (Hall et al., 2002; Hall and Riggs, 2007; Wang et al., 2008; Parajka et al., 2012; Hou et al., 2018; Liu et al., 2020). The MODIS snow cover algorithm and products are also the foundation of the Visible Infrared Imaging Radiometer Suite (VIIRS) snow cover algorithms, ensuring the accuracy, continuity and consistency of the resulting snow cover datasets from the Suomi-National Polar-orbiting Partnership (S-NPP), Joint Polar Satellite System-1 (JPSS-1, now known as NOAA-20) and JPSS-2 (now known as NOAA-21) (Riggs et al., 2017; Riggs and Hall, 2020; Liu A. et al., 2022; Stillinger et al., 2023; Román et al., 2024). According to the research by Zhang H. et al. (2020), the VNP10A1 product from VIIRS performs as well as the MOD10A1 product from Terra, except on the Tibetan Plateau, and is significantly more accurate than the MYD10A1 data from Aqua in China. It is recommended to prioritize the use of snow cover products from VIIRS and Terra rather than snow cover products from Aqua because of the questionable observations of Band 6 in Aqua (Huang et al., 2018; Hall et al., 2019; Zhang H. et al., 2020). In addition, S-NPP VIIRS produced the VNP46A1 and VNP46A2 products using nighttime light remote sensing data, achieving a classification accuracy exceeding 79% in Arctic ice and snow cover monitoring scenarios (Liu et al., 2023). The AVHRR snow cover products provided by the European Space Agency (ESA) achieved an overall accuracy of 94% in the Himalayas (Wu et al., 2021). The JASMES product, which was developed using NOAA AVHRR and MODIS data, attained an accuracy exceeding 82% (Hori et al., 2017). Since 2008, China's FY-3 series satellites, which are equipped with a Medium Resolution Spectral Imager (MERSI), Visible and InfraRed Radiometer (VIRR) and Microwave Radiation Imager (MWRI), have provided critical Earth observations. The accuracy of the multisensor fusion snow cover products (MULSS) derived from the FY-3 MERSI and VIRR data ranges from 83% to 87%, reflecting long-term snow cover trends in China (Min et al., 2021; Li et al., 2022). Optical and passive microwave imagery derived from the FY-3D MERSI and MWRI has also been integrated to generate new snow cover products, known as MULSS\_SCM. In addition to the aforementioned snow cover products with spatial resolutions ranging from hundreds of meters to several kilometers, satellite data with spatial resolutions as fine as tens of meters are also available. For example, the United States Geological Survey (USGS) provides Landsat-8 L3-level data with a 30 m resolution and a 16-day temporal interval for the fractional Snow Covered Area (fSCA). The F1-score, the harmonic mean of precision and recall, for the Landsat-8 products reached 97.3%, slightly outperforming the metrics of MODIS and VIIRS, as validated by airborne lidar datasets in the western USA (Stillinger et al.,



2023). With respect to Sentinel-2 satellites, which have a high spatial resolution of 20 m, the empirical threshold-based method of the official processor (Sen2Cor) has achieved an overall accuracy of only 58% (Wang et al., 2022c). In contrast, enhanced Let-It-Snow (LIS) algorithms and machine learning methods, such as random forests and U-Net models, can increase this accuracy to 90%–94% (Barrou Dumont et al., 2021; Richiardi et al., 2021;

Li et al., 2022). The Theia Snow Collection provides high-resolution snow cover maps (20–30 m) using Sentinel-2 and Landsat-8 data by incorporating the NDSI and snow lines. These maps serve as valuable references for evaluating MODIS snow cover products and data assimilation methods. The Sentinel-2 results from the Theia Snow Collection have achieved an overall accuracy of 94% and a kappa coefficient of 0.83 (Gascoin et al., 2019). Additionally, these

TABLE 1 Prominent snow cover products derived from polar-orbiting satellites.

Satellites	Optical sensor	Launch year	Spatial resolution	Temporal resolution	Snow cov	er product
	MODIS	1999/2002	500 m	1 d	MOD10A1/MYD10A1; MOD10A1F/MYD10A1F	
				8 d	MOD10A2/MYD10A2	
Terra/Aqua			5 km	1 d	MOD10C1/MYD10C1	
				8 d	MOD10C2/MYD10C2	
				Monthly	MOD10CM/MYD10CM	
a Naba (abas a labas a	VIIRS	2011/2017/2022	375 m	1 d	VNP10A1/VJ110A1; VNP10A1F/VJ110A1F	
S-NPP/JPSS-1/JPSS-2			500 m	1 d	VNP46A1; VNP46A2	
NOAA series satellites	AVHRR	1979	5 km	1 d	JASMES; SnowCCI AVHRR products	
Landsat series satellites	TM/ETM+/OLI	1984	30 m	16 d	Theia Snow	Landsat SCA/fSCA
Sentinel-2	MSI	2015	20 m	20 m 5 d		HRSI collection
		2008	1 km	1 d	MERSI/MULSS SNow Cover (SNC)	
FY-3	MERSI		5 km	1 d	FY-3 MULSS Snow O	Cover Merged (SCM)

Sentinel-2 results are more sensitive to *in situ* SD observations than are those of MODIS, as the optimal SD threshold for the former is close to 0 m, whereas for MODIS, the optimal SD threshold is 0.15 m, at which the product achieves its best kappa coefficient (Gascoin et al., 2015; Gascoin et al., 2019). All the abovementioned snow cover products, which are available at different spatial and temporal resolutions, offer diverse data support for snow monitoring at both global and regional scales.

Therefore, snow cover reconstruction methods must be selected while carefully considering the detection characteristics of different satellites or constellations. For example, temporal methods that rely on continuous multiday snow cover information are challenging to apply to Landsat and Sentinel-2 products with low temporal resolutions. When nighttime light remote sensing data are utilized for snow cover monitoring in polar regions, it is essential to account for the impact of lunar phase changes on image brightness, and methods must be employed to remove clouds and auroras (Liu et al., 2023). Snow cover products with various spatial resolutions require different reconstruction strategies. For daily products with moderate spatial resolutions ranging from 1 km to 5 km (Table 1), the primary objective of snow cover reconstruction is to retrieve snow information obscured by cloud cover. For Landsat and Sentinel-2 satellite products, which have high spatial resolutions (<30 m) and long revisit intervals, daily snow cover maps may need to be generated using temporal interpolation methods, along with cloud gap filling. These factors illustrate the variations exhibited by snow cover reconstruction methods across different spatiotemporal scales and emphasize the significance of satellite observation characteristics in snow reconstruction algorithms.

Therefore, research on snow cover reconstruction must adopt more precise methods to increase the clear-sky accuracy and quality of the original products. Furthermore, the resolutions of snow cover products and their detection characteristics should be considered when an appropriate snow cover reconstruction method is selected.

### 3 Snow cover reconstruction methods

Snow cover reconstruction methods, which are also referred to as cloud removal approaches, are employed primarily to fill data gaps caused by cloud cover, cloud shadows, forest cover or detector saturation in snow cover products. These methods increase the reliability and continuity of snow cover products, facilitating their application in runoff forecasting and data assimilation systems (Hall et al., 2010; Coll and Li, 2018; Hall et al., 2019; Li et al., 2020). Numerous researchers have conducted relevant studies on snow cover reconstruction based on the distinct characteristics of snow cover products. We classified snow cover reconstruction methods according to their predominant use for BSC and NDSI/FSC products in existing studies to better reflect common practices. Some methods—such as certain machine learning algorithms—classified under NDSI/FSC reconstruction have also been applied to BSC products and, in some cases, have generated both types of results simultaneously. Nevertheless, we still categorize them as NDSI/FSC methods to encourage the generation of continuousvalue outputs, which preserve more detailed snow information and can be readily converted to BSC products through appropriate thresholding.

## 3.1 Reconstruction methods for BSC products

Based on the different gap-filling principles, the snow cover reconstruction methods that are commonly used for BSC products can be classified into temporal filters, spatial filters, multisource fusion, and the hidden Markov random field (HMRF) model (Coll and Li, 2018; Li X. et al., 2019; Gao Y. et al., 2024). As BSC products remain valuable data sources for large-scale snow monitoring and satisfy snow cover detection needs at coarse resolutions, these methods continue to evolve. In this paper, we provide a concise review of these methods.

There are four types of commonly used temporal filters: Terra and Aqua combination (TAC), adjacent temporal deduction (ATD), fixed and flexible multiday combination (MDC), and the snow cycle filter (SCFil). These methods are based on the temporal continuity of snow cover and the dynamic processes of snow accumulation and ablation. They assume that snow cover undergoes minimal change over certain periods, whereas cloud cover changes more rapidly. As a result, clouds can be effectively removed by combining multitemporal snow cover products within a temporal window. The typical size of this temporal window ranges from several hours (TAC) to tens of days (Liang TG. et al., 2008; Parajka and Blöschl, 2008; Gao et al., 2010b; Singh et al., 2021; Mattar et al., 2022; Wang J. et al., 2025). Generally, a larger temporal window reduces cloud contamination but also decreases the overall classification accuracy and temporal resolution. Therefore, selecting appropriate temporal windows for different regions and seasons is essential for balancing cloud removal efficiency with classification accuracy, ultimately improving the overall quality of the data. Gao et al. (2010b) reported that underestimation and overestimation errors typically remain low during stable snow-covered and nonsnow periods (generally December-March and July-September, depending on regional snow characteristics) when TAC, ATD, and MDC are used with temporal windows ≤8 days. However, larger temporal windows in the fixed MDC method result in increased overestimation errors during transitional periods. In contrast, the flexible MDC method provides an effective solution for improving reconstruction outcomes by adjusting the window size based on cloud cover percentage and a predefined maximum number of days (Gao et al., 2010b; Zhang et al., 2012; Chen et al., 2014; Yang et al., 2018). Notably, temporal filters are ineffective at completely removing clouds from BSC products, except for SCFil. However, the error of SCFil is the greatest among these methods, exceeding 10% (Gafurov and Bárdossy, 2009; Li X. et al., 2019). The SCFil method assumes that snow cover persists between the start day of snow accumulation and the day of complete snowmelt, during which all the cloud pixels are reclassified as snow-covered. In contrast, cloud pixels are classified as snow-free during other periods. The SCFil method is constrained by the accuracy of the estimated snow start and complete snowmelt days. Overall, the performance of the method is influenced by cloud cover dynamics and may be further diminished during periods of rapid snow change. Previous research has demonstrated that the SCFil method tends to overestimate snow cover on land pixels (Gafurov and Bárdossy, 2009). These temporal filters are generally suitable for scenes with frequent dynamic interference (e.g., clouds and auroras) and relatively stable snow cover. The higher the frequency of satellite observations is, the more effective the temporal filters are (Liang TG. et al., 2008; Parajka and Blöschl, 2008; Gafurov and Bárdossy, 2009; Gao et al., 2010b; Paudel and Andersen, 2011; Lindsay et al., 2015; Singh et al., 2021; Liu et al., 2023). Short-term snowfall or snowmelt events can reduce the accuracy of temporal filtering methods.

The spatial filters are primarily based on four orthogonal neighboring pixels, the elevation of eight neighboring pixels, locally weighted logistic regression (LWLR), and snow lines. Spatial filters rely primarily on snow cover information and the environmental association information of neighboring pixels within a specific spatial window to reclassify cloud pixels. Spatial filters based on four orthogonal neighboring pixels or the elevation of eight neighboring pixels achieve high classification accuracy but remove only a few cloud pixels (Gafurov and Bárdossy, 2009; Jain et al., 2009; Tong et al., 2009; Paudel and Andersen, 2011; López-Burgos et al., 2013; Grünewald et al., 2014; Hou et al., 2018; Li X. et al., 2019; Poussin et al., 2025). The LWLR method can reduce the cloud coverage rate from 39% to 15% (López-Burgos et al., 2013) but exhibits significant temporal variations, with unstable cloud removal effects and high computational costs (Clark and Slater, 2006; López-Burgos et al., 2013). Different snow-line methods estimate snow and land boundaries in different ways based on snow distributions to reclassify cloud pixels (Guglielmin et al., 2003; Gafurov and Bárdossy, 2009; Parajka et al., 2010; Paudel and Andersen, 2011; Qiu et al., 2017; Zhang et al., 2023). The most commonly used snow-line method is the regional snowline method (SNOWL) (Parajka et al., 2010; Dietz et al., 2014; Hüsler et al., 2014; Poussin et al., 2025), which is affected by the misclassification of cloud pixels as snow cover pixels and does not account for cloud shadows, making it difficult to apply this technique to snow cover products derived from high-spatialresolution satellites such as Landsat-8 and Sentinel-2. Therefore, Zhang et al. (2023) enhanced the SNOWL algorithm using the tools Fmask and Sen2Cor to identify cloud cover, cloud shadows and snow pixels precisely in Sentinel-2 images. Additionally, unstable snow cover areas were incorporated to improve the snow cover reconstruction process in mountainous regions affected by clouds and cloud shadows, making the method more suitable for Sentinel-2 data (Zhang et al., 2023; Zhang et al., 2024). Considering that snow cover is influenced by various factors, Qiu et al. (2017) also employed multiple linear regression to model snow-line elevation data for reconstruction purposes, using the snow-line elevation as the dependent variable and the longitude, latitude and slope aspect as independent variables. This method has been widely applied to conduct snow monitoring over the Qinghai-Tibet Plateau and the China-Pakistan Economic Corridor (Qiu et al., 2017; Yu, 2017; Hao et al., 2019). However, both the improper selection of subregions and the overfitting of regressions affect the cloud removal rate and classification accuracy of this method. In general, the above spatial filters perform best in areas with simple terrain and stable snow cover conditions over a wide range. They generally perform well in filling gaps caused by small, scattered clouds but are less effective in areas with extensive cloud cover (Huang et al., 2018; Yan et al., 2024).

Traditional multisource fusion methods involve the combination of BSC products derived from optical observations, SD or SWE products acquired from passive microwave

observations, and station observations. Owing to the coarse spatial resolution of microwave products, the SWE or SD needs to be sampled to align them with the spatial resolution of BSC products, and cloud pixels in BSC products are directly replaced with the corresponding reclassified SWE pixels (Liang T. et al., 2008; Gao et al., 2010a; Gao et al., 2010b; Foster et al., 2011; Bergeron et al., 2014; Huang et al., 2016; Romanov, 2017; Hao et al., 2021). Station observations provide continuous, long-term and high-precision SD data but are limited to fixed locations. Therefore, integrating station observations with remote sensing products requires the consideration of additional spatial distribution characteristics of snow (Gafurov et al., 2015; Dong and Menzel, 2016; Gafurov et al., 2016). When remote sensing images are scarce, the reconstruction of long time series and large-scale historical snow cover can be accomplished by constructing a probabilistic relationship between individual pixels and station data. However, data quality differences caused by the migration of ground stations, environmental changes, observation standard revisions, and unstable operations may negatively impact the accuracy of snow cover fusion products (Yang et al., 2013; Zhang et al., 2021). Additionally, some researchers have proposed integrating IMS snow and ice products with BSC products, as IMS products offer higher spatial resolutions (1–4 km) and can serve as alternatives to microwave products (Newfel et al., 2013; Li Y. et al., 2019; Gao Z. et al., 2024; Hao et al., 2019; Wang J. et al., 2025). With the development of nighttime light remote sensing, the combination of snow cover products from both daytime and nighttime has shown significant promise in snow cover reconstruction. High spatial resolution snow cover products derived from VIIRS nighttime light data can be used not only for polar night monitoring but also as valuable complements to conventional optical products (such as MODIS BSC products). The integration of both daytime and nighttime products can reduce cloud cover by more than 30% and expand the observation range (Chen et al., 2023). Applying multiple temporal and spatial filters to reduce the number of cloud pixels before using multisource fusion methods can help minimize the degree of uncertainty in snow cover monitoring tasks (Newfel et al., 2013; Huang et al., 2014; Li Y. et al., 2019; Zheng and Cao, 2019; Wang et al., 2022a).

The HMRF model is a widely used framework for image segmentation tasks; it accounts for the mutual influences of adjacent observations and expresses a contextual relationship (Dubes and and Jain, 1989; Chatzis and Tsechpenakis, 2010). The HMRF model for snow cover reconstruction aims to integrate spectral, spatial, temporal, and environmental information; calculate the total spatiotemporal energy (probability) for each cloud pixel; and determine whether the target pixel corresponds to a snow or nonsnow pixel (Huang et al., 2018; Huang et al., 2022b). This method effectively and efficiently removes cloud cover from snow cover products, enhancing the cloud removal process during periods with unstable snow and in complex terrain areas. This method has demonstrated strong performance on both the MODIS and AVHRR datasets (Huang et al., 2018; Hao et al., 2021; Hao et al., 2022; Wang, 2022; Huang and Xu, 2022; Gao Y. et al., 2024; Hao et al., 2025; Wang Q. et al., 2025). Additionally, Huang et al. (2022b) incorporated solar radiation as environmental background information into the HMRF method, replacing the conventional process of using surface elevation data. This approach more effectively captures the combined influence of factors such as slope, aspect and sunlight duration. Increased solar radiation results in a delayed onset of snow cover, faster snowmelt, and more rapid snow cover changes (Dombrovsky and Kokhanovsky, 2022). As a result, the HMRF method, which incorporates solar radiation, reduces commission and omission errors, with overall accuracies ranging from 0.91 to 0.98.

Among these approaches, temporal filters, spatial filters and multisource fusion are limited by insufficient cloud removal capabilities or reduced accuracy and are often combined into multistep methods to generate cloud-free BSC products. The HMRF method simultaneously accounts for the spatiotemporal correlation of snow cover, fully utilizing both spatial and temporal information to restore missing data. The HMRF model can be employed for snow cover reconstruction either independently or in combination with other methods.

### 3.2 Reconstruction methods for the NDSI and FSC products

NDSI and FSC products are also commonly used snow cover products derived from optical remote sensing data. Unlike BSC products, NDSI and FSC products provide continuously varying snow parameters. NDSI or FSC values can be converted to BSC products using an appropriate threshold (such as NDSI = 0.5 or FSC = 0.4), after which snow cover can be reconstructed via the methods described in Section 3.1. However, the NDSI and FSC provide more detailed snow cover information and are being increasingly used directly in related studies. Temporal and spatial interpolation methods, spatiotemporal reconstruction algorithms, machine learning-based reconstruction algorithms and data assimilation can be applied to NDSI and FSC data.

#### 3.2.1 Temporal and spatial interpolation methods

The simplest reconstruction methods for NDSI or FSC products are temporal and spatial interpolation methods, which evolve from temporal and spatial filters for BSC products. They still rely on the temporal or spatial continuity of snow cover, but each method considers only one of these characteristics at a time.

The temporal interpolation methods for NDSI or FSC products assume that the FSC gradually changes over a short period. Therefore, the predicted FSC value of a cloud pixel can be interpolated from FSC values within a temporal window. Like the TAC method used for BSC products, combining Terra and Aqua MODIS NDSI/FSC products represents a specific application of temporal interpolation methods. This approach typically uses maximum value composition, averaging, or valid-value selection from the two MODIS products-often prioritizing the more accurate Terra products (e.g., MOD10A1) when available (Hou et al., 2019; Qiu and Wang, 2021; Hou et al., 2022). Hou et al. (2019) applied a more general method, adjacent temporal filtering (ATF), which replaced cloud-covered pixels with the nearest cloud-free FSC value from the previous 3 days. Similarly, Hou et al. (2022) used a variant of the ATF, averaging the NDSI values from adjacent days to fill missing pixels. Pan et al. (2024) replaced cloud pixels on the current day with the arithmetic mean of the observed FSC values on the previous and following days. Poussin et al. (2025) integrated data from Sentinel-2 and Landsat satellites to

generate monthly composites by selecting the maximum NDSI value for each pixel across all available images. Additionally, the linear interpolation, quadratic interpolation, cubic spline interpolation (CSI) or piecewise cubic Hermite interpolating polynomial (PCHIP) can be applied to clear-sky values within a fixed or adaptively changing temporal window to estimate the NDSI and FSC values for cloud pixels in segments (Dozier et al., 2008; Tang et al., 2013; Hao et al., 2014; Hou et al., 2022; Deng et al., 2024b; Hua et al., 2025). However, the interpolation algorithm, which considers only the temporal continuity of snow cover, lacks sufficient effective data during extended periods of cloudy weather, making the interpolated values prone to outliers.

Spatial interpolation methods estimate NDSI or FSC values based on the values of cloud-free pixels surrounding a cloud pixel. If most of the neighboring pixels around a cloud pixel have valid values, the cloud pixel is assigned the interpolated value of the snow-covered neighboring pixels. In the simplest case, the FSC value of a cloud pixel is the arithmetic mean of the effective FSC values of four or eight neighboring pixels (Pan et al., 2024). In addition, the inverse distance weight (IDW) interpolation algorithm within the selected spatial window also performs effectively. Researchers can further screen cloud-free pixels with appropriate altitude differences within the spatial window for IDW interpolation, leading to a mean absolute error of 0.10 in the FSC results (Pan et al., 2024). Like spatial filters, complex terrain and environmental factors can cause anomalies in the interpolation results.

#### 3.2.2 Spatiotemporal reconstruction algorithms

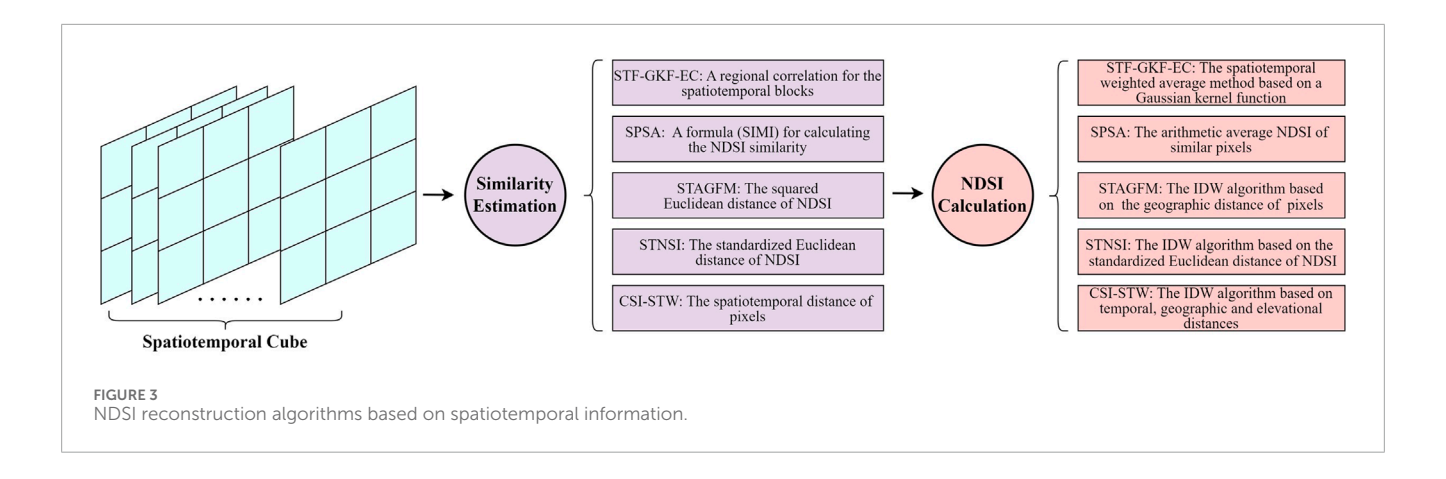
Spatiotemporal reconstruction algorithms aim to reconstruct NDSI or FSC values at cloud pixels by jointly leveraging the temporal and spatial continuity of snow cover. Unlike approaches that rely on only one of these dimensions, they simultaneously integrate both and are sometimes further refined with auxiliary topographic information such as DEM. These algorithms consider snow cover information within a spatiotemporal cube or image pairs from multiple dates.

To fully leverage the spatiotemporal snow cover information of a single product, five reconstruction algorithms can be employed to generate cloud-free NDSI or FSC products. These include a spatiotemporal fusion method based on the Gaussian kernel function and error correction (STF-GKF-EC) (Jing et al., 2019; Jing et al., 2022), a spatiotemporal similar pixel selecting algorithm (SPSA) (Li et al., 2020), a spatial and temporal adaptive gap-filling method (STAGFM) (Chen et al., 2020), a spatiotemporal cube cloud removal algorithm based on NDSI similarity (STNSI) (Guo et al., 2024), and a spatiotemporal weighted method combined with CSI (CSI-STW) (Deng et al., 2024b). These methods generally follow similar principles: treating the target cloud pixel as the central pixel, determining similarity estimation rules, selecting the clearsky pixels with the highest similarity to the central pixel from the dynamic spatiotemporal cube, and calculating the NDSI of the central pixel by weighting the NDSI of the most similar clear-sky pixels based on their spatiotemporal distances (Figure 3).

Each method estimates similarity differently, but they all assume that similar pixels have similar NDSI values, consistent multitemporal changes, and spatial proximity overall. The STF-GKF-EC method primarily uses a regional correlation coefficient (greater than 0.7) for the spatiotemporal blocks within a temporal

window to select similar pixels. It subsequently employs a Gaussian kernel function to perform spatiotemporal weighted averaging on the selected similar pixels, thereby estimating the NDSI for cloud pixels (Jing et al., 2019). This method was enhanced to form the Spatio-Temporal Adaptive fusion method with erroR correction (STAR), which produces an NDSI collection with reduced omission errors (Jing et al., 2022). The SPSA provides a formula  $(SIMI_p^p)$ for calculating the NDSI similarity between pixels and incorporates multiyear variations as a constraint for predicting the NDSI value at a cloud pixel. Several clear-sky pixels with the highest similarity values are selected, and their arithmetic average NDSI is used to replace the cloud pixel (Li et al., 2020). STAGFM calculates the squared Euclidean distance of the NDSI between the central pixel and its spatially neighboring clear-sky pixels, selecting those with the smallest distances as similar pixels. The NDSI of the target cloud pixel can be predicted by a weighted average of the bias-corrected NDSI values of similar pixels, where the contribution of a pixel is inversely proportional to its geographic distance (Chen et al., 2020). The STNSI method is somewhat similar to the STAGFM method, but it calculates NDSI differences and average NDSI errors for performing correction within a snow season rather than at the target and reference images, as in the STAGFM method (Guo et al., 2024). The CSI-STW method places greater emphasis on the spatiotemporal correlation of snow cover and incorporates elevation control conditions to constrain the process of selecting similar pixels (Deng et al., 2024b). It employs the Inverse Distance Weighted (IDW) method to reconstruct the NDSI of cloud pixels, with their weights determined by their temporal, geographic and elevational distances. In these methods, spatiotemporal cubes that are too small may limit the number of similar pixels available for reconstruction, whereas overly large cubes can significantly increase computational costs. Consequently, typical spatiotemporal cube sizes range from  $3 \times 3 \times t$  to  $5 \times 5 \times t$ , where t usually spans 5–17 days (Jing et al., 2022; Deng et al., 2024b; Guo et al., 2024). Additionally, the STAGFM algorithm adopts a 15 × 15 spatial window and selects 20 similar pixels to achieve optimal accuracy (Chen et al., 2020). Future research may explore the use of dynamically adaptive window sizes to more effectively balance reconstruction accuracy and computational efficiency.

addition to the aforementioned spatiotemporal reconstruction methods employed for single remote sensing products, some studies have explored the complementary spatiotemporal characteristics of multisource images and developed spatiotemporal fusion algorithms for generating high-accuracy and high-resolution snow products. Unlike spatiotemporal reconstruction algorithms for individual products, spatiotemporal fusion algorithms evaluate the similarity between pixels of coarse and fine products using a sliding window and calculate the transformation coefficients based on spatiotemporal weights. The coarse-resolution products are downscaled and integrated with the fine-resolution products. For example, Bousbaa et al. (2022) selected ESTARFM, FSDAF and preclassification FSDAF from various spatiotemporal data fusion algorithms (Zhu et al., 2010; Zhu et al., 2016) and combined Sentinel-2 and Landsat-8 images to generate 10-m NDSI products, effectively filling data gaps caused by cloud cover and cloud shadows. The root mean square error (RMSE) of the fused NDSI generated by the preclassification FSDAF algorithm was only 0.12, demonstrating the highest accuracy. Because the



preclassification FSDAF algorithm employs a supervised machine learning technique instead of the unsupervised classification process used in FSDAF, it obtains more accurate input BSC data as a constraint for spatiotemporal fusion. This approach effectively integrates spatiotemporal fusion methods with machine learning. Gao et al. (2022) developed an enhanced spatiotemporal fusion method, iESTARFM, for integrating Landsat and MODIS products. This method distinguishes snow pixels from non-snow pixels using NDSI and DEM thresholds and calculates similarity values based on pixel categories. The iESTARFM algorithm achieved a correlation coefficient greater than 0.9 in the visible and near-infrared bands, indicating a high level of agreement with the actual conditions and enhancing the accuracy of the NDSI calculations. Dong et al. (2024) employed the FSDAF method to integrate MODIS and Sentinel-2 data, generating daily NDSI products at a 20-m spatial resolution. Their findings indicate that the reliability of the FSDAF model in regions with persistent cloud cover requires further investigation, as the NDSI values were significantly underestimated in heavily clouded areas. This highlights the importance of further enhancing cloud removal and NDSI reconstruction during the spatiotemporal integration process. Xiao et al. (2024) developed a spatiotemporal fusion framework that integrates microwave data with MODIS optical data to generate 1-km daily FSC products, achieving overall accuracies of 0.92-0.94 across various land covers, including grasslands, wetlands, farmlands, and urban areas. Guo et al. (2025) employed the ESTARFM algorithm to combine MODIS and Sentinel-2 NDSI, producing 10-m NDSI products and enhancing the accuracy of snow cover mapping in the eastern Qilian Mountains. These fusion algorithms aim to integrate both coarse and fine products, improve temporal and spatial resolution, enhance reconstruction accuracy, and increase applicability. However, their explanations of complex environmental factors remain insufficient, and their accuracies are influenced by the selection of reference images from both products in algorithm construction.

Spatiotemporal reconstruction algorithms typically require similarity evaluations between pixels in remote sensing spatiotemporal images, and their overall accuracy generally exceeds 90%. However, less prior snow information becomes available when cloud coverage persists for longer periods, reducing the accuracy of spatiotemporal reconstruction algorithms. Although methods such as CSI-STW have been optimized for use under prolonged cloudy conditions, they still struggle to account for complex factors

such as slope, aspect, land cover, and vegetation cover. Extremely rapid and fluctuating snow variations may introduce errors during reconstruction, leading to inconsistencies between the selected similar pixels and cloud pixels. Additionally, the accuracy of original snow cover products inherently constrains the performance of reconstruction algorithms. Applying machine learning techniques to snow cover identification, extracting accurate prior information, and subsequently reconstructing snow cover can be effective strategies for improving the accuracy of reconstructed NDSI or FSC products (Zhu et al., 2016; Bousbaa et al., 2022; Gao et al., 2022).

### 3.2.3 Machine learning-based reconstruction algorithms

Advancements in image processing and computing technology have enabled machine learning to introduce innovative strategies for reconstructing snow cover.

First, machine learning-based reconstruction methods can further analyze the spatiotemporal characteristics of snow cover, efficiently incorporate auxiliary environmental data such as meteorological and geographic information, and increase the accuracy of reconstructed snow cover products. For example, Hou et al. (2019) developed a nonlocal spatiotemporal filtering (NSTF) algorithm via the fast elitist nondominated sorting genetic algorithm for multi-objective optimization (NSGA-II) (Hou and Huang, 2016). The NSTF algorithm integrates MODIS snow products with geographic information, including land cover, elevation, slope and aspect information, to reconstruct snow cover. This method retained 0.52% of the cloud cover while achieving an overall accuracy of 93.7%, outperforming the CSI method. Xing et al. (2022) proposed a U-Net model with partial convolutions (PU-Net) that utilizes spatiotemporal information to reconstruct the MODIS NDSI, achieving an MAE of less than 0.15 under simulated conditions. However, heterogeneous and rapidly changing snow cover reduces the reconstruction accuracy of PU-Net, and the absence of auxiliary data, such as topography and temperature, limits its performance. Hou et al. (2022) developed three methods based on long short-term memory (LSTM) deep neural networks, namely, forward, backward and bidirectional LSTM, and applied them to reconstruct MODIS NDSI products by following the TAC method. This study revealed that the bidirectional LSTM model performed best, enabling snow cover reconstruction to be implemented in complex mountainous regions by learning temporal

NDSI features and incorporating spatially assisted information derived via the IDW. The overall accuracy of this method reached 89.9% in the source region of the Yellow River. Yatheendradas and Kumar (2022) utilized topographic, precipitation, SWE, leaf area index, MODIS snow albedo and surface temperature data as input variables. A three-layer legacy superresolution convolutional neural network (SRCNN) was trained to reconstruct the snow cover in the MOD10A1 dataset. This method can produce snow cover reconstructions even when data gaps are inconsistent across multisource datasets, enabling its widespread application. Zhu (2022) developed a snow grain size gap-filling model based on a spatiotemporal extra tree by utilizing geographical and meteorological information acquired from the Kaidu River Basin. The results indicated that among the seven widely used machine learning methods, the spatiotemporal extra tree achieved the most effective reconstruction effect, reducing the annual average cloud coverage level by approximately 18% compared with that of MOD10A1 products (Zhu et al., 2023). Xiao et al. (2021) applied Random Forest (RF) in combination with optical and passive microwave data to avoid the influences of cloud contamination and estimate the FSC. Their work inspired Du (2024) to apply the RF model to generate binary snow cover maps using brightness temperature data and MODIS reference products, demonstrating its effectiveness in reconstructing nighttime snow cover and mitigating overestimation in high-altitude regions. In addition, when machine learning is integrated with high-resolution (1–5 m) satellite images, the vegetation index and other auxiliary data enhance the snow monitoring capabilities of the utilized algorithms in challenging areas, including canopy edges, forest gaps, and even areas beneath dense canopies. This advancement is crucial for improving the snow cover reconstruction process in forested regions (John et al., 2022; Yang et al., 2023). Additionally, Ye et al. (2024) proposed a spatiotemporal extreme gradient boosting (STXGBoost) model to generate a gap-filled NDSI dataset, achieving a mean absolute error of 0.011 by incorporating multisource auxiliary data, including surface albedo. Dong et al. (2025) developed a LightGBM-based NDSI reconstruction method, suggesting that the incorporation of snow-related spatiotemporal and environmental information significantly improved the quality and accuracy of the reconstructed products. In addition to the models mentioned above, the application of Transformer models in image reconstruction has recently attracted increasing interest from researchers. Xu et al. (2025) proposed the MAT-MS model, which employs a Swin Transformer-based encoder and a CNN-based decoder, integrating topographic and temperature data to reconstruct the MODIS NDSI. Furthermore, MAT-MS incorporates a novel mask-aware technique to address inaccuracies and mitigate unnatural transitions at data gap boundaries. Compared with the CNN, LSTM, and U-Net models, the MAT-MS model demonstrates superior performance, with average MAE and RMSE values of 1.585 and 5.531, respectively.

Second, when machine learning techniques are applied to snow cover reconstruction tasks, they can perform spatiotemporal downscaling simultaneously, thereby significantly increasing the availability and applicability of snow cover products. For example, Wang et al. (2022b) developed the STDFA-matching-Pix2pix-GAN (SMPG) algorithm, which integrates a spatial-temporal data fusion approach (STDFA) with the pix2pixGAN to fuse MODIS and Landsat images, compute the NDSI, and generate daily snow cover

maps with a spatial resolution of 30 m. A performance evaluation against four benchmark methods-STARFM, FSDAF, SwinSTFM (Swin spatiotemporal fusion model), and GAN-STFM (GANbased spatiotemporal fusion model)—demonstrates the superior performance of SMPG, which effectively reduces the spectral distortion of the fused images and achieves the highest average correlation coefficient of 0.962. Richiardi et al. (2023) developed a two-stage RF algorithm to integrate MODIS and Sentinel-2 products, generating daily cloud-free snow cover products at a spatial resolution of 20 m and providing both NDSI and BSC values. In this method, the first-stage RF model fills the gaps observed in the MODIS products, whereas the second-stage RF model performs multisource data fusion and downscaling. The overall accuracy of the generated products exceeded 92%. Zakeri and Mariethoz (2024) employed the K-nearest neighbor (KNN) classification algorithm, which integrates meteorological data to address the low temporal resolutions of Landsat and Sentinel-2 data and produces high-resolution daily snow cover images at 30 m. This method generates both BSC and NDSI products. A comprehensive analysis indicated that machine learning reconstruction algorithms achieve multisource data fusion and downscaling, effectively mitigating the limitations posed by cloud contamination in high-spatial-resolution remote sensing data (e.g., Landsat-8/9 or Sentinel-2 data). These approaches typically provide products with the highest spatiotemporal resolution, enabling the precise monitoring of snow cover dynamics (Revuelto et al., 2021; Rittger et al., 2021; Kollert et al., 2024).

reconstruction, machine To achieve learning-based reconstruction algorithms can rapidly integrate geographic information, meteorological observations and weather forecasts alongside spatiotemporal information of snow cover. These algorithms incorporate meteorological and climatic factors that influence snow accumulation and snowmelt processes rather than relying solely on the spatiotemporal distribution of snow cover, as is done in spatiotemporal reconstruction algorithms. As a result, machine learning-based reconstruction algorithms can not only generate high-precision and high-resolution cloud-free snow cover products but also enable the historical reconstruction and future prediction of snow cover in scenarios that lack remote sensing observations, thus demonstrating significant application potential (Koehler et al., 2022). However, machine learning typically relies on high-quality training samples that adequately represent the characteristics of the target domain. Inadequate sample size, excessive noise, or overly complex model structures can lead to overfitting, whereas overly simplistic models or insufficient features may result in underfitting. A sufficient quantity of highquality training samples and optimized network architectures are crucial for improving the generalizability of machine learning-based algorithms. For example, Hou et al. (2022) reported that 21 hidden layer nodes in their bidirectional LSTM-based algorithm optimally balanced underfitting (with fewer nodes) and overfitting (with more nodes) for snow cover reconstruction. Moreover, challenges such as persistent snow cover, cloud cover, varying training time spans, and different land cover types further complicate machine learning-based reconstruction efforts (Hou et al., 2019; Dong et al., 2025). Therefore, the generalizability of machine learning models to large-scale snow monitoring scenarios worldwide, as well as their reconstruction accuracy under complex surface conditions, requires

further testing and evaluation (Hou et al., 2022). Although effective in multisource data processing, these models face interpretability challenges. Researchers often conduct extensive literature reviews before modeling to identify candidate input variables based on snow physical characteristics. Because many factors influence snow distribution, considering all of them is impractical, and excessive variables may reduce model generalizability. Current strategies include manually determining and testing different variable combinations (John et al., 2022; Ye et al., 2024), progressively incorporating additional data sources (Xu et al., 2025), applying importance-based feature selection (Xiao et al., 2021; Dong et al., 2025), and using SHAP analysis to improve interpretability. Zhu et al. (2023) demonstrated that altitude, as the most influential topographic factor, had the highest importance score (0.192). Xu et al. (2025) reported that incorporating DEM into their MAT-MS model significantly improved performance, reducing the RMSE by 0.611. For Dong et al. (2025), the top five ranked variables were spatiotemporal interpolation, shortwave radiation, cumulative shortwave radiation over 3 days, latitude, and elevation.

In general, the effective combination of remote sensing data, meteorological data and machine learning has promoted the advancement of snow cover reconstruction methods, resulting in higher accuracy and improved product resolution. This approach is expected to provide better cloud-free snow cover products for meteorological and hydrological models.

#### 3.2.4 Data assimilation methods

Data assimilation (DA) methods feed remote sensing-based snow cover products into hydrological, land surface, meteorological, and climate models, accounting for consistency constraints as well as physical and dynamic properties (Pandya et al., 2022). This approach improves the simulation of snow cover parameters and facilitates snow cover reconstruction. DA methods include direct insertion (DI), Cressman interpolation, optimal interpolation (OI), the ensemble Kalman filter (EnKF), and the particle filter (PF), among others. OI and the EnKF are the most common snow data assimilation methods (Helmert et al., 2018). In recent years, the particle batch smoother (PBS) has also been widely used to conduct data assimilation on MODIS snow cover observations, making it well suited for simulating snow cover in data-scarce regions (Alonso-González et al., 2021).

Researchers have conducted extensive research on snow data assimilation. One of the most notable examples is the American Snow Data Assimilation System (SNODAS) (Barrett, 2003). Since 2003, the SNODAS system has provided daily snow products at a 1-km resolution for the United States and its surrounding regions and is widely utilized because of its strong real-time performance. The system primarily integrates meteorological information derived from numerical weather prediction models and the NOHRSC Snow Model (NSM) and employs a simple nudging or Newtonian relaxation procedure to assimilate satellite, airborne and groundbased snow cover observations (Barrett, 2003; Vuyovich et al., 2014; Lv et al., 2019). Owing to the insufficient representation of blowing snow processes and snow interception by forest canopies in the NSM, SNODAS results in significant deviations in certain regions (Vuyovich et al., 2014; Lv et al., 2019). Lv et al. (2019) demonstrated that further assimilating SNODAS products into the Cold Region Hydrological Model (CRHM) could effectively increase

the accuracy of snow cover estimation. With advancements in DA, various innovative approaches have emerged. Arsenault et al. (2013) assimilated MOD10A1 into the Community Land Model (CLM2) using the DI and the EnKF, respectively, revealing accuracy differences across various altitudes. Zhang et al. (2023) developed a multivariate land snow data assimilation system for the Northern Hemisphere that integrates the Data Assimilation Research Testbed (DART) and CLM4. After the MODIS snow cover products were assimilated, the system exhibited reduced errors in snow parameters such as the FSC and SD (Zhang and Yang, 2016). In addition, the NASA High Mountain Asia Team (HiMAT) developed a Bayesian snow reanalysis framework and employed the PBS method to assimilate snow cover data derived from Landsat and MODIS, producing the High Mountain Asia (HMA) Snow Reanalysis (HMASR) dataset (Margulis et al., 2019; Liu et al., 2021). By utilizing the HMASR as a reference to evaluate eight global snow cover datasets, the study revealed that the global datasets generally underestimated the peak snow storage levels in HMA (Liu Y. et al., 2022). As reported by Fiddes et al. (2019), assimilating MODIS products via the PBS method improved the accuracy of snow cover estimation at multiple spatial scales and reduced the biases induced during downscaling processes. Similarly, the snow reanalysis product (ICAR\_assim) produced by Alonso-González et al. (2021) employs the PBS method and strongly agrees with gap-filled snow cover products derived from MODIS data. Subsequently, Alonso-González et al. (2022) developed the Multiple Snow Data Assimilation System (MuSA), which incorporates six data assimilation algorithms, including the EnKF. In MuSA computational benchmarks, different data assimilation algorithms exhibit substantial variation in computational cost. Overall, those derived from the EnKF are more time-consuming than those derived from the PF. For instance, when the computational cost of the PBS, measured in wall-clock time, is 39s, that of EnKF-MDA reaches 270s (Alonso-González et al., 2022). MuSA enables the joint assimilation of FSC and land surface temperature (LST) products derived from MODIS, which can enhance the snow cover monitoring and reconstruction processes in the absence of sunlight during the polar night, as the LST provides supplementary thermodynamic information (Thiebault and Young, 2020; Alonso-González et al., 2022). More importantly, MuSA is an opensource collaborative project that is conducive to promoting further research on the topic of snow. MuSA has been used in snow cover simulations over the Heihe River Basin, assimilating the MODIS NDSI product into the Flexible Snow Model, effectively filling data gaps and reducing errors in snow cover monitoring (Deng et al., 2024a). In addition, reanalysis datasets (e.g., ERA5, MERRA-2, and NCEP/NCAR) can provide snow parameters, including snow cover. However, the accuracy of snow monitoring is not optimal without specific optimization of snow cover (Brown et al., 2010; Baba et al., 2021). Generally, the complexity of data assimilation and models affects their computational efficiency, particularly in high-resolution and large-scale snow cover monitoring scenarios, where a rational method selection process is essential.

In general, snow data assimilation aims to comprehensively assess the properties of snow and generate high-precision, gridded snow parameters, including snow cover, SD, SWE and snow density. Additionally, it systematically evaluates the uncertainties associated with models, algorithms and data products. Snow cover

reconstruction is merely one of the outcomes of DA. Given the significant potential of integrating remote sensing observations with numerical models, DA represents a crucial direction for the future development of snow monitoring and forecasting techniques (Girotto et al., 2020; Alonso-González et al., 2022).

#### 4 Validation and evaluation methods

### 4.1 Reference data for validation and evaluation

The validation and evaluation of snow cover reconstruction datasets constitute critical steps in demonstrating the reliability and robustness of reconstruction methods in snow cover research. Various types of reference data can be used for this purpose, including *in situ* SD observations, snow cover maps, field survey measurements, and airborne lidar datasets.

*In situ* SD observations are a primary source of reference data for validating and evaluating snow cover reconstruction datasets. These measurements are typically collected from regional meteorological stations (Qiu et al., 2017; Huang et al., 2018; Hou et al., 2018; Hou et al., 2019; Huang et al., 2022b), Natural Resources Conservation Service (NRCS) Snow Telemetry (SNOTEL) sites (Gao et al., 2010b; López-Burgos et al., 2013; Huang et al., 2018), or ground-based GNSS stations (Hua et al., 2025). For validation purposes, SD values should be converted into a binary snow/non-snow format, with thresholds typically set at 1 cm or 3 cm. Values exceeding the selected threshold are classified as snow-covered, whereas those below are considered non-snow. The number and temporal coverage of stations are determined by the specific requirements of the study. Depending on the study area and the density of stations, the number of stations can range from a few to several thousand. Stations with substantial amounts of invalid data may be excluded, and additional screening may be applied where appropriate (Dong et al., 2025). For example, Pan et al. (2024) excluded stations with SD values greater than 1 cm but fewer than 20 snow-covered days to better illustrate the accuracy of snow identification. The validation period can range from several months to multiple decades and may cover the entire year or focus solely on snow seasons on an annual basis. However, a scale mismatch exists between point-based station observations and pixel-based snow cover products (Hall et al., 2019), and the spatial distribution of meteorological stations is often highly uneven. Stations are primarily concentrated in lowelevation valleys with human settlements, whereas high-elevation snow-covered regions remain sparsely monitored (Li et al., 2020). Therefore, in situ station data alone cannot adequately represent entire regions, making evaluation based on snow cover maps necessary to validate the spatial accuracy of snow cover products (Richiardi et al., 2023).

Evaluation based on snow cover maps generally follows two main approaches. The first involves the use of snow cover maps derived from other sources, such as higher-resolution products generated from Landsat, Sentinel, or GF satellite imagery through clear-sky NDSI calculations, or existing datasets such as IMS products (Dietz et al., 2014; Huang et al., 2018; Huang et al., 2022b; Richiardi et al., 2023; Zhang et al., 2023; Zhu et al., 2023; Deng et al.,

2024b; Guo et al., 2024; Pan et al., 2024; Zhang et al., 2024; Xu et al., 2025). These snow cover maps are resampled to match the spatial resolution of the reconstructed snow cover products. The second approach is based on the cloud mask assumption. In this method, cloud masks are extracted from original cloudy remote sensing images and applied to cloud-free images, which are regarded as the ground truth (Gafurov and Bárdossy, 2009; Hou et al., 2019; Li et al., 2020; Chen et al., 2020; Xing et al., 2022; Dong et al., 2025). The reconstruction results are subsequently generated from the masked images and compared with the original cloud-free images for evaluation.

Field survey measurements refer to snow data collected during *in situ* snow observation experiments within the study area, whereas airborne LiDAR datasets are obtained from Airborne Snow Observatory (ASO) campaigns (Stillinger et al., 2023; Yang et al., 2023). Field measurements and airborne remote sensing campaigns require substantial resources. Although these datasets are highly reliable and valuable, they are difficult to obtain and are often constrained in both temporal and spatial coverage.

### 4.2 Evaluation metrics and validation results

For BSC products, commonly used evaluation metrics include overall accuracy (OA), precision (PC), recall (RC), F1-score, and the Kappa coefficient (Table 2; Equations 1–5). Additional metrics, such as MU and MO, are employed to represent underestimated and overestimated snow events (Equations 6, 7) (Qiu et al., 2017; Xing et al., 2022; Zhu et al., 2023; Dong et al., 2025). When using SD data from *in situ* stations, survey measurements, or airborne lidar datasets to validate reconstructed NDSI/FSC products, the SD values must first be converted into binary snow cover (BSC) format before validation is conducted.

$$OA = (TP + TN) \div (TP + TN + FP + FN) \times 100\%$$
 (1)

$$PC = TP \div (TP + FP) \times 100\% \tag{2}$$

$$RC = TP \div (TP + FN) \times 100\% \tag{3}$$

$$F1 - score = 2 \times PC \times RC \div (PC + RC) \times 100\%$$
 (4)

Kappa = 
$$\frac{p_o - p_e}{1 - p_e}$$
,  
 $p_o = OA, p_e = \frac{(TP + FP)(TP + FN) + (FN + TN)(FP + TN)}{(TP + TN + FP + FN)^2}$  (5)

$$MU = FN \div (TP + TN + FP + FN) \times 100\%$$
 (6)

$$MO = FP \div (TP + TN + FP + FN) \times 100\% \tag{7}$$

When the NDSI/FSC products are validated using snow cover maps, the commonly used metrics include the coefficient of determination  $(R^2)$ , root mean square error (RMSE), mean absolute error (MAE), correlation coefficient (r), and mean difference error

TABLE 2 Confusion matrix comparing reconstructed products with reference data.

Reference Reconstruction	Snow	Non-snow
Snow	TP	FP
Non-snow	FN	TN

(Bias) (Equations 8–12) (Hou et al., 2019; Hou et al., 2022; Zhu et al., 2023; Ye et al., 2024; Dong et al., 2025).

$$R^{2} = 1 - \frac{\sum_{i=1}^{n} (S_{ref}^{i} - S_{rec}^{i})^{2}}{\sum_{i=1}^{n} (S_{ref}^{i} - \overline{S_{ref}})^{2}},$$
 (8)

RMSE = 
$$\sqrt{\frac{\sum_{i=1}^{n} (S_{rec}^{i} - S_{ref}^{i})^{2}}{n}}$$
, (9)

$$MAE = \frac{1}{n} \sum_{i=1}^{n} \left| S_{rec}^{i} - S_{ref}^{i} \right|$$
 (10)

$$r = \frac{\sum_{i=1}^{n} (S_{ref}^{i} - \overline{S_{ref}}) (S_{rec}^{i} - \overline{S_{rec}})}{\sqrt{\sum_{i=1}^{n} (S_{ref}^{i} - \overline{S_{ref}})^{2} \sum_{i=1}^{n} (S_{rec}^{i} - \overline{S_{rec}})^{2}}}$$
(11)

$$Bias = \frac{1}{n} \sum_{i=1}^{n} \left( S_{rec}^{i} - S_{ref}^{i} \right)$$
 (12)

where n denotes the number of sample pixels,  $S_{rec}^{i}$  and  $S_{ref}^{i}$  represent the NDSI/FSC values of the i th pixel in the reconstructed product and the reference dataset, respectively, and  $\overline{S_{rec}}$  and are the corresponding mean NDSI/FSC values.

To further account for spatial accuracy, a bias-insensitive metric called spatial efficiency (SPAEF, Equation 13) (Hou et al., 2019) and Robert's edge detection (Equation 14) have been used for snow cover spatial evaluation (Dong et al., 2025). The SPAEF metric integrates three components: the correlation coefficient (A) between the reconstructed and reference images, the fraction of the coefficient of variation (B), and the percentage of histogram intersection (C); an optimal SPAEF value of 1 indicates perfect agreement between the two images. For Robert's edge evaluation,  $D_{x,y}$  denotes the pixel value at the x th row and y th column; a value of 0 represents a perfectly fused image, negative values indicate excessive smoothing of edge features, and positive values indicate oversharpening (Zhu et al., 2022).

$$SPAEF = 1 - \sqrt{(A-1)^2 + (B-1)^2 + (C-1)^2}$$
 (13)

Edge = 
$$|D_{x,y} - D_{x+1,y+1}| + |D_{x,y+1} - D_{x+1,y}|$$
 (14)

These evaluation metrics facilitate cross-method validation experiments, and some of the results are summarized in Tables 3, 4. Compared with the temporal CSI method, the NSTF-based method achieved OA, MU, and MO values that were 2% higher, 1.92% lower, and 0.04% lower, respectively (Hou et al., 2019). The spatiotemporal extra tree method of Zhu et al. (2023) and the HRMF-based method of Hao et al. (2022) each excelled on different validation dates;

the former generally performed better on days 3 and 4. Moreover, the LightGBM-based method proposed by Dong et al. (2025) achieved an OA of around 83-86% and an F1-score of 53-61%, outperforming the CGF NDSI (Deng et al., 2024b) and matching the performance of the STAR NDSI (Jing et al., 2022). Compared with the spatiotemporal interpolation (SI) method, the LightGBM-based method also showed improved numerical and spatial accuracy with an R<sup>2</sup> of 0.82 and an Edge of -0.47. Wang et al. (2025b) evaluated four snow cover reconstruction methods: MOD10A1F, the HMRFbased method (Hao et al., 2022), the STAR method (Jing et al., 2022), and the stepwise cloud-removal approach (Qiu and Wang, 2021). They found that the HMRF-based product consistently delivered the best performance, and the STAR product's performance varied with terrain complexity and cloud conditions. In comparison, the stepwise cloud-removal approach generally performed the worst. Under the most challenging conditions, its F1-score dropped to as low as 41.2%, whereas the other methods maintained F1-scores in the range of 63-68%. These validation and evaluation results suggest that, while the HMRF model, spatiotemporal reconstruction algorithms (e.g., STAR), and machine learning-based algorithms may each have advantages under different conditions, they generally outperform simpler methods such as temporal and spatiotemporal interpolation.

#### 5 Discussion

Snow cover products derived from polar-orbiting satellites offer extensive global coverage, high spatial resolution, and broad applicability, making them indispensable for global snow cover monitoring. However, factors such as cloud cover, cloud shadows, forest cover and undetected data often result in data gaps in snow cover products. Consequently, reconstruction methods are needed to restore snow cover information, enhancing the reliability and continuity of snow cover products. This strategy provides comprehensive and accurate data support for studies on climate change and related fields.

The essence of snow cover reconstruction lies in inferring and estimating the values of uninformative pixels using existing observational data. Reconstruction methods typically analyze the spatiotemporal distribution characteristics of snow cover to impose additional assumptions that constrain the estimated values of cloud-covered pixels (Figure 4). They may also incorporate multisource snow observations to fill data gaps or integrate various auxiliary environmental variables that influence snow accumulation and melt—such as solar radiation, slope, aspect, land cover type, topographic relief index (TRI), topographic position index (TPI), temperature and precipitation—to enrich the information available for reconstruction. Accordingly, reconstruction accuracy improves with more stable spatiotemporal snow cover characteristics, more realistic assumptions, greater availability of multisource data, and more effective data utilization.

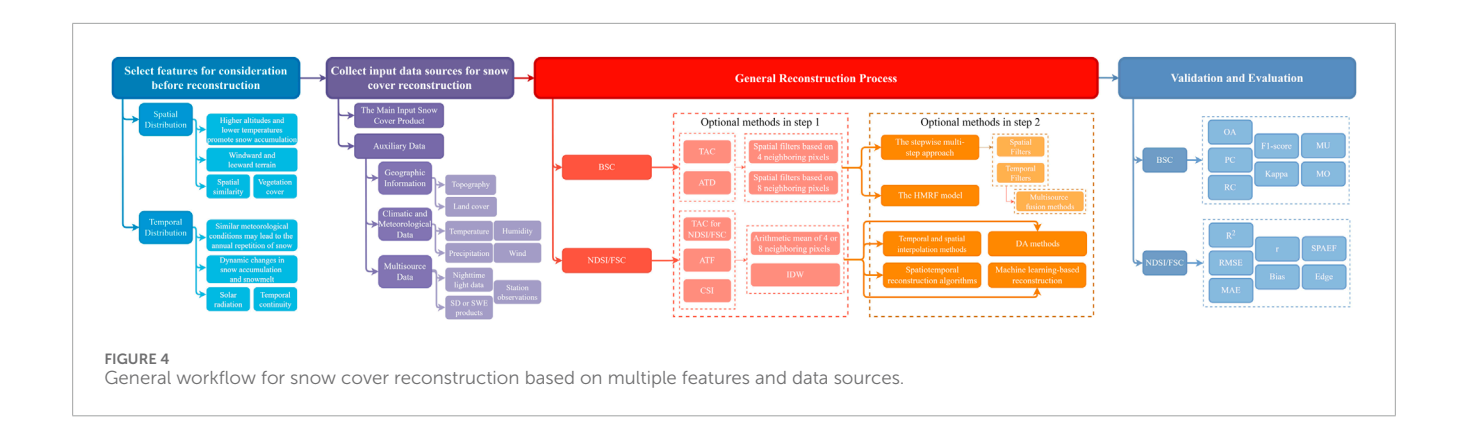
For the BSC and NDSI/FSC products, each snow cover reconstruction method has specific applications, along with their respective characteristics (Table 5). According to previous studies, temporal and spatial filters, multisource fusion methods, and temporal and spatial interpolation methods are generally straightforward and easy to implement, making them suitable

TABLE 3 Comparison between the NSTF-based method and the temporal CSI method (compiled from Hou et al., 2019; CC BY 4.0).

Rese	earch	Methods	Validation Data	Time Range	Study Area	ОА	MU	МО
***	1 (2010)	The proposed NSTF-based method	No. 1 1 10 1 10 0 0 1 10 0 0 1		N. d. W	87	6.85	6.30
Hou et al. (2019)		The temporal CSI method	Meteorological Stations' SD Observations	2001—2016	North Xinjiang	85	8.77	6.34

TABLE 4 Comparison between the methods based on the spatiotemporal extra tree and the HMRF model (adapted from Zhu et al., 2023; CC BY 4.0).

Research	Methods	Validation Data	Time Range	Study Area	OA	PC	RC	F1-score	Карра
Zhu et al. (2023)	The proposed spatiotemporal extra tree model  The HRMF-based method (Hao et al., 2022)	Cloud Assumption of Original Snow Cover Data	8 October 2015 20 April 2016 25 April 2018 1 June 2018	Kaidu River Basin	92.89 86.99 91.44 95.77 94.43 92.58 89.45 94.96	70.12 87.55 80.34 73.13 75.23 78.54 69.02 63.72	90.40 54.69 90.84 76.21 87.65 91.52 96.62 65.80	78.98 67.32 85.27 74.64 80.97 84.53 80.52 64.75	74.78 59.74 79.26 72.33 77.72 79.69 73.56 62.03



for monitoring remote sensing data at medium and low spatial resolutions (≥1 km) over large stable snow cover areas. While the computational complexity of the HMRF model, spatiotemporal reconstruction algorithms, machine learning-based methods, and data assimilation techniques is relatively high, these approaches generally yield more stable results. Among them, spatiotemporal reconstruction algorithms enhance accuracy by thoroughly exploring the spatiotemporal similarity among snow-covered pixels and weighting the contributions of similar pixels accordingly. However, these algorithms depend primarily on the snow cover products themselves and the assumption of spatiotemporal consistency. Their limited use of auxiliary data—aside from elevation—reduces their effectiveness under unstable conditions, such as prolonged cloud cover or rapidly fluctuating snow dynamics. In contrast, the HMRF model, machine learning-based methods, and data assimilation techniques typically incorporate a richer set of environmental variables as input features or explicitly account for them in the modeling process. Therefore, in complex terrains with strong snow heterogeneity, limited observations, nighttime conditions, or forested regions—where other methods tend to underperform—these approaches often yield more accurate and robust monitoring results. Notably, the distinction between snow cover reconstruction methods for BSC and NDSI/FSC products is not absolute. For instance, reconstructed NDSI/FSC products can be converted into BSC outputs using appropriate thresholds, whereas certain methods developed for NDSI/FSC reconstruction may likewise be adapted for binary snow cover estimation with appropriate modifications. Moreover, reconstruction approaches designed for either BSC or NDSI/FSC products may inspire the development of methods for the other product type.

In practice, most studies employ more than one method to achieve snow cover reconstruction. For example, Gafurov and Bárdossy (2009) proposed a six-step procedure involving TAC, MDC, SNOWL, spatial filters based on four and eight neighboring pixels, and SCFil. Huang et al. (2018) applied an HMRF-based spatiotemporal modeling approach after merging Terra and Aqua snow products. Wang J. et al. (2025) developed a four-step method of TAC, ATD, spatial filters, and the integration of MODIS and

TABLE 5 Characteristics and applicability of snow cover reconstruction methods.

Products	Snow cover reconstruction methods	Complete cloud removal	Applicability and suggestions
BSC	Temporal Filters	Generally, no	(1) Temporal filters are suitable for relatively stable snow-covered regions with dynamic phenomena, such as clouds and aurora.  (2) The original snow cover products must have high temporal resolution (typically 1 day).  (3) TAC and ATD are recommended as preprocessing steps before applying other snow cover reconstruction methods.  (4) SCFil completely removes all cloud pixels, but its accuracy is relatively low. The use of this method needs to be carefully considered.
	Spatial Filters	No	<ul> <li>(1) Spatial filters are suitable for open landscapes with simple terrain, uniform land cover (such as large expanses of bare soil), and stable snow cover.</li> <li>(2) The original products should have moderate or low cloud cover rates and high spatial resolution (preferably ≤1 km).</li> <li>(3) Spatial filters based on four or eight neighboring pixels generally have low cloud removal rates. They are not recommended for use alone but can serve as preprocessing steps before applying other methods.</li> </ul>
	Multisource Fusion Methods	Yes	(1) The combination of BSC and SD/SWE products is suitable for open scenes with stable snow cover and relatively low spatial resolution requirements. This method can be used as the final step after applying other methods to address the remaining cloud pixels. (2) The combination of remote sensing and station observations reconstructs historical datasets in remote mountainous regions with limited observations. (3) The combination of daytime and nighttime snow cover products represents a promising development direction due to the high resolution of the products.
	HMRF	Yes	It has broad applicability and is suitable for mountainous regions with unstable snow cover and complex terrain, such as the Qinghai-Tibet Plateau.
NDSI/FSC	Temporal and Spatial Interpolation Methods	Generally, no	The application of these methods is similar to that of temporal and spatial filters. They are better suited as preprocessing steps before applying other snow cover reconstruction methods.
	Spatiotemporal Reconstruction Algorithms	Yes	(1) These reconstruction algorithms are commonly used for NDSI or FSC products when only snow cover products are available, with little or no geographic data (such as land use or DEM).  (2) The spatiotemporal fusion method facilitates the integration of both coarse and fine products, improving reconstruction accuracy and enhancing applicability.
	Machine Learning-Based Reconstruction Algorithms	Yes	(1) These methods can rapidly utilize auxiliary spatiotemporal and environmental information. They have broad applicability and potential, particularly in areas with complex terrain, forest cover, and at night.  (2) When a high spatiotemporal resolution is needed, this type of method can be used to conduct downscaling work through the introduction of multiple auxiliary datasets.  (3) A reliable reference derived from actual observations must be used for training and testing.

(Continued on the following page)

TABLE 5 (Continued) Characteristics and applicability of snow cover reconstruction methods.

Products	Snow cover reconstruction methods	Complete cloud removal	Applicability and suggestions
	Data Assimilation Methods	Yes	(1) Their applicability is broad. Considering the computational cost, these methods are recommended for regions with rapid snow cover changes and complex terrain or surfaces. (2) They are suitable for conducting research on various snow properties beyond snow cover, such as the SD, SWE and snow grain size.

IMS data to generate a daily snow cover dataset for Central Eurasia. Poussin et al. (2025) employed a seven-step gap-filling procedure that included SNOWL and spatial filters. Dong et al. (2025) first used TAC to reduce missing pixels and then used a spatiotemporal cube neighborhood interpolation method to construct spatiotemporal features, followed by filling missing NDSI values with a LightGBM model. This multistep strategy varies depending on several factors. First, some methods, although reasonably accurate, cannot completely remove the clouds. These methods, including most temporal and spatial filters as well as temporal and spatial interpolation methods, must be combined with other methods to remove cloud contamination step by step until no cloud-covered pixels remain. Second, multisource fusion methods have the problems of inconsistent accuracy and scale among multiple data sources. If used, they are usually placed as the last step to mitigate the impacts. The HMRF model, spatiotemporal reconstruction algorithms and machine learning-based methods consider various factors simultaneously and can achieve complete cloud removal. However, researchers prefer to use appropriate combinations of TAC, ATD, and spatial filters based on four neighboring pixels for BSC products and simple temporal and spatial interpolation methods for NDSI/FSC products as preprocessing steps before using the HMRF model, spatiotemporal reconstruction algorithms or machine learning-based methods. These methods are simple and easy to implement, and their accuracy is relatively high. The most crucial point is that they can initially reduce a portion of the missing information as a constraint for subsequent processing. Excessive lack of information may increase the risk of generating extreme outliers. Although errors may accumulate across multiple steps, most of these errors are acceptable when compared with the potential extreme outliers.

The future development of snow cover reconstruction techniques can be approached from three perspectives: snow cover observations, characteristics and reconstruction methods. First, with respect to observations, the accuracy of the original snow cover products needs to be enhanced. The snow cover reconstruction process heavily depends on prior information about the original snow cover products. Although the accuracy of many original products has been validated using station observations, the regional representativeness of these stations is limited, and errors caused by misclassifications and omissions continue to impact the reconstruction results. Therefore, more stringent strategies must be implemented to extract snow cover from satellite spectral images to maximize the accuracy of snow recognition (Zhu et al., 2016; Bousbaa et al., 2022; Gao et al., 2022). Approaches may include developing novel deep learning models, exploring the

potential of deep semantic segmentation networks for cloud-snow discrimination, creating automated and adaptive snow detection methods with dynamic adjustment for seasonal and regional variability, and integrating spectral and texture features for improved snow identification (Han L. et al., 2019; Wu et al., 2019; Wang et al., 2022d; Wang et al., 2023; Ding et al., 2024). Second, based on an analysis of snow cover characteristics, the effectiveness of a snow cover reconstruction procedure relying solely on a single characteristic is typically suboptimal. During the process of snow cover reconstruction, comprehensively considering complex terrain, temperature, precipitation, solar radiation, vegetation cover, and other spatial and temporal environmental factors can significantly improve the accuracy and resolution of the reconstruction results. As a result, multisource heterogeneous data, which provide rich spatial and temporal environmental information, will become crucial supplements. However, several issues persist, including spatial and temporal resolution discrepancies, geographical positioning differences and the high processing complexity associated with multisource products. It is essential to thoroughly evaluate the reliability of multisource data while strengthening the data quality control and verification processes. In addition, ensuring the alignment, correction and unified processing of multisource data is crucial. This can be achieved through feature identification, appropriate transformations and resampling, orthorectification, geometric correction, and super-resolution techniques (Samadzadegan et al., 2025). Standardized preprocessing, multilevel (pixel, feature, and decision) data fusion, and open, shared snow datasets for algorithm validation and comparison can further enhance the effectiveness of multisource data fusion (Ghamisi et al., 2019; Samadzadegan et al., 2025; Yang et al., 2025). Among the various snow cover reconstruction methods, machine learningbased reconstruction algorithms and DA are being increasingly recognized as important techniques because of their significant advantages in processing multisource data. These methods can not only efficiently process multisource data independently but also have the potential for integration. For example, the cost function employed in four-dimensional variational data assimilation (4D-Var) is equivalent to the loss function used by neural networks, both of which can be unified under a Bayesian framework. This theoretical commonality enables the integration of machine learning and DA (Geer, 2021). Machine learning can complement DA by performing tasks such as model error correction, parameter estimation, and observation bias correction. In turn, DA provides physical constraints for machine learning, thereby mitigating the associated overfitting issues. The combination of these two methods can maximize the utilization of increasing remote sensing

observations, harmonize data with various resolutions to generate gridded products, and enhance both the estimation and prediction of snow cover and the related snow characteristics while also resulting in improved computational efficiency. This integrated approach offers a novel perspective for snow cover monitoring and forecasting in complex environments, with significant potential for broader application.

#### 6 Conclusion

Snow cover reconstruction methods have made significant progress in addressing data gaps in snow cover products derived from polar-orbiting satellites. Traditional approaches, such as temporal and spatial filters, multisource fusion methods, and temporal and spatial interpolation methods, remain effective for large-scale applications, whereas emerging techniques, such as HMRF models, spatiotemporal algorithms, machine learning, and data assimilation, demonstrate potential in complex environments. Method selection depends on product resolution, snow characteristics, cloud contamination, and the balance between accuracy and computational cost, with hybrid approaches often proving most effective. Future developments should focus on three key directions. First, improving snow detection algorithms to enhance the quality of baseline products is a prerequisite for reliable reconstruction. Second, topography, climate, vegetation, and other spatiotemporal environmental factors should be systematically integrated, and comprehensive multisource data fusion frameworks should be constructed, while strengthening quality control and uncertainty assessment. Third, the integration of machine learning and data assimilation methods should be advanced to maximize the value of expanding remote sensing datasets. To support future research and algorithm development in snow cover reconstruction, a list of open-access datasets and related source codes of potential interest to researchers is provided in the Appendix of the Supplementary file. Progress in these areas will enable the production of gridded, gap-free snow products that are reliable, accessible, and user-friendly, supporting snow monitoring across diverse environments. Overall, this review provides a foundation for long-term monitoring and detailed analysis of snow cover, offering critical support for research on the cryosphere and water resources.

#### **Author contributions**

JZ: Writing – review and editing, Resources, Conceptualization. XZ: Formal Analysis, Investigation, Writing – review and editing, Writing – original draft. JW: Writing – review and editing, Formal Analysis, Methodology. JL: Writing – review and editing. ZX: Writing – review and editing, Conceptualization, Project administration.

#### **Funding**

The author(s) declare that financial support was received for the research and/or publication of this article. This research was supported by China Yangtze Power Co., Ltd under Grant [number Z242302024]. The funder was not involved in the study design, collection, analysis, interpretation of data, the writing of this article, or the decision to submit it for publication.

### Acknowledgments

The authors would like to thank Zhaojun Zheng of the National Satellite Meteorological Center (National Centre for Space Weather) for helpful discussions on this work.

#### Conflict of interest

Author JZ was employed by China Yangtze Power Co., Ltd.

The remaining authors declare that the research was conducted in the absence of any commercial or financial relationships that could be construed as a potential conflict of interest.

#### Generative AI statement

The author(s) declare that Generative AI was used in the creation of this manuscript. The authors used ChatGPT solely to improve the language and subsequently reviewed and edited the content to ensure accuracy and clarity.

Any alternative text (alt text) provided alongside figures in this article has been generated by Frontiers with the support of artificial intelligence and reasonable efforts have been made to ensure accuracy, including review by the authors wherever possible. If you identify any issues, please contact us.

#### Publisher's note

All claims expressed in this article are solely those of the authors and do not necessarily represent those of their affiliated organizations, or those of the publisher, the editors and the reviewers. Any product that may be evaluated in this article, or claim that may be made by its manufacturer, is not guaranteed or endorsed by the publisher.

### Supplementary material

The Supplementary Material for this article can be found online at: https://www.frontiersin.org/articles/10.3389/feart.2025.1649808/full#supplementary-material

#### References

Alonso-González, E., Gutmann, E., Aalstad, K., Fayad, A., Bouchet, M., and Gascoin, S. (2021). Snowpack dynamics in the Lebanese mountains from quasi-dynamically downscaled ERA5 reanalysis updated by assimilating remotely sensed fractional snow-covered area. *Hydrol. Earth Syst. Sci.* 25 (8), 4455–4471. doi:10.5194/hess-25-4455-2021

Alonso-González, E., Aalstad, K., Baba, M. W., Revuelto, J., López-Moreno, J. I., Fiddes, J., et al. (2022). The multiple snow data assimilation system (MuSA v1.0). *Geosci. Model Dev.* 15 (24), 9127–9155. doi:10.5194/gmd-15-9127-2022

Armstrong, R. L., Rittger, K., Brodzik, M. J., Racoviteanu, A., Barrett, A. P., Khalsa, S.-J. S., et al. (2019). Runoff from glacier ice and seasonal snow in High Asia: separating melt water sources in river flow. *Reg. Environ. Change* 19 (5), 1249–1261. doi:10.1007/s10113-018-1429-0

Arsenault, K. R., Houser, P. R., De Lannoy, G. J. M., and Dirmeyer, P. A. (2013). Impacts of snow cover fraction data assimilation on modeled energy and moisture budgets. *J. Geophys. Res. Atmos.* 118 (14), 7489–7504. doi:10.1002/jgrd.50542

Baba, M. W., Boudhar, A., Gascoin, S., Hanich, L., Marchane, A., and Chehbouni, A. (2021). Assessment of MERRA-2 and ERA5 to model the snow water equivalent in the high Atlas (1981–2019). *Water* 13 (7), 890. doi:10.3390/w13070890

Barrett, A. P. (2003). National operational hydrologic remote sensing center SNOw data assimilation system (SNODAS) products at NSIDC NSIDC special Report 11. Boulder, CO, USA: National Snow and Ice Data Center. Available online at: https://nsidc.org/sites/default/files/nsidc\_special\_report\_11.pdf.

Barrou Dumont, Z., Gascoin, S., Hagolle, O., Ablain, M., Jugier, R., Salgues, G., et al. (2021). Brief communication: evaluation of the snow cover detection in the copernicus high resolution snow & ice monitoring service. *Cryosphere* 15 (10), 4975–4980. doi:10.5194/tc-15-4975-2021

Bergeron, J., Royer, A., Turcotte, R., and Roy, A. (2014). Snow cover estimation using blended MODIS and AMSR-E data for improved watershed-scale spring streamflow simulation in Quebec, Canada. *Hydrol. Process.* 28 (16), 4626–4639. doi:10.1002/hyp.10123

Bousbaa, M., Htitiou, A., Boudhar, A., Eljabiri, Y., Elyoussfi, H., Bouamri, H., et al. (2022). High-resolution monitoring of the snow cover on the Moroccan atlas through the spatio-temporal fusion of Landsat and sentinel-2 images. *Remote Sens. (Basel).* 14, 5814. doi:10.3390/rs14225814

Brown, R., Derksen, C., and Wang, L. (2010). A multi-data set analysis of variability and change in Arctic spring snow cover extent, 1967–2008. *J. Geophys. Res. Atmos.* 115 (D16). doi:10.1029/2010jd013975

Chatzis, S. P., and Tsechpenakis, G. (2010). The infinite hidden Markov random field model. *IEEE Trans. Neural Netw.* 21 (6), 1004–1014. doi:10.1109/tnn.2010.2046910

Chen, S., Wang, X., Guo, H., Xie, P., and Sirelkhatim, A. M. (2020). Spatial and temporal adaptive gap-filling method producing daily cloud-free NDSI time series. *IEEE J. Sel. Top. Appl. Earth Observations Remote Sens.* 13, 2251–2263. doi:10.1109/jstars.2020.2993037

Chen, S., Yang, Q., Xie, H., Zhang, H., Lu, P., and Zhou, C. (2014). Spatiotemporal variations of snow cover in northeast China based on flexible multiday combinations of moderate resolution imaging spectroradiometer snow cover products. *J. Appl. Remote Sens.* 8 (1), 084685. doi:10.1117/1.jrs.8.084685

Chen, B., Zhang, X., Ren, M., Chen, X., and Cheng, J. (2023). Snow cover mapping based on SNPP-VIIRS day/night band a case study in Xinjiang, China. *Remote Sens.* 15 (12), 3004. doi:10.3390/rs15123004

Clark, M. P., and Slater, A. G. (2006). Probabilistic quantitative precipitation estimation in complex terrain. *J. Hydrometeorol.* 7 (1), 3–22. doi:10.1175/jhm474.1

Coll, J., and Li, X. (2018). Comprehensive accuracy assessment of MODIS daily snow cover products and gap filling methods. *ISPRS J. Photogrammetry Remote Sens.* 144, 435–452. doi:10.1016/j.isprsjprs.2018.08.004

Da Ronco, P., and De Michele, C. (2014). Cloud obstruction and snow cover in Alpine areas from MODIS products. *Hydrol. Earth Syst. Sci.* 18 (11), 4579–4600. doi:10.5194/hess-18-4579-2014

Deng, G., Liu, X., Shen, Q., Zhang, T., Chen, Q., and Tang, Z. (2024a). Remote sensing data assimilation to improve the seasonal snow cover simulations over the Heihe River Basin, northwest China. *Int. J. Climatol.* 44 (15), 5621–5640. doi:10.1002/joc.8656

Deng, G., Tang, Z., Dong, C., Shao, D., and Wang, X. (2024b). Development and evaluation of a cloud-gap-filled MODIS normalized difference snow index product over High Mountain Asia. *Remote Sens.* (*Basel*). 16, 192. doi:10.3390/rs16010192

Dietz, A. J., Kuenzer, C., Gessner, U., and Dech, S. (2012). Remote sensing of snow – a review of available methods. *Int. J. Remote Sens.* 33 (13), 4094–4134. doi:10.1080/01431161.2011.640964

Dietz, A. J., Conrad, C., Kuenzer, C., Gesell, G., and Dech, S. (2014). *Identifying changing snow cover characteristics in central Asia between 1986 and 2014 from remote sensing data. Remote Sens.* 6 (12), 12752–12775. doi:10.3390/rs61212752

Ding, L., Xia, M., Lin, H., and Hu, K. (2024). Multi-level attention interactive network for cloud and snow detection segmentation. *Remote Sens.* 16 (1), 112. doi:10.3390/rs16010112

Dixit, A., Goswami, A., and Jain, S. (2019). Development and evaluation of a new "snow water index (SWI)" for accurate snow cover delineation. *Remote Sens.* 11 (23), 2774. doi:10.3390/rs11232774

Dobreva, I. D., and Klein, A. G. (2011). Fractional snow cover mapping through artificial neural network analysis of MODIS surface reflectance. *Remote Sens. Environ.* 115 (12), 3355–3366. doi:10.1016/j.rse.2011.07.018

Dombrovsky, L. A., and Kokhanovsky, A. A. (2022). Deep heating of a snowpack by solar radiation. *Front. Therm. Eng.* 2, 882941. doi:10.3389/fther.2022.882941

Dong, C., and Menzel, L. (2016). Producing cloud-free MODIS snow cover products with conditional probability interpolation and meteorological data. *Remote Sens. Environ.* 186, 439–451. doi:10.1016/j.rse.2016.09.019

Dong, L., Zhou, H., Xu, J., Tang, Y., Teng, X., Ni, J., et al. (2024). BI or IB: which better generates high spatiotemporal resolution NDSI by fusing sentinel-2A/B and MODIS data? *IEEE J. Sel. Top. Appl. Earth Observations Remote Sens.* 17, 3314–3333. doi:10.1109/jstars.2023.3347202

Dong, L., Zhou, H., Gu, Q., Xu, J., Hua, R., Yu, B., et al. (2025). A novel approach for cloud-free MODIS NDSI reconstruction on the Tibetan plateau combining spatiotemporal cube and environmental features. *IEEE Trans. Geoscience Remote Sens.* 63, 1–14. doi:10.1109/tgrs.2025.3542095

Dozier, J., and Warren, S. G. (1982). Effect of viewing angle on the infrared brightness temperature of snow. *Water Resour. Res.* 18 (5), 1424–1434. doi:10.1029/wr018i005p01424

Dozier, J., Painter, T. H., Rittger, K., and Frew, J. E. (2008). Time-space continuity of daily maps of fractional snow cover and albedo from MODIS. *Adv. Water Resour.* 31 (11), 1515–1526. doi:10.1016/j.advwatres.2008.08.011

Du, J. (2023). Snow mapping from passive microwave brightness temperature and MODIS snow product with machine learning approaches. (master's thesis). University of Waterloo. Available online at: https://uwspace.uwaterloo.ca/items/3e595db9-0882-4455-b748-8a8a826f669a.

Dubes, R. C., and And Jain, A. K. (1989). Random field models in image analysis. *J. Appl. Statistics* 16 (2), 131–164. doi:10.1080/02664768900000014

Fiddes, J., Aalstad, K., and Westermann, S. (2019). Hyper-resolution ensemble-based snow reanalysis in mountain regions using clustering. *Hydrol. Earth Syst. Sci.* 23 (11), 4717–4736. doi:10.5194/hess-23-4717-2019

Foster, J. L., Hall, D. K., Eylander, J. B., Riggs, G. A., Nghiem, S. V., Tedesco, M., et al. (2011). A blended global snow product using visible, passive microwave and scatterometer satellite data. *Int. J. Remote Sens.* 32 (5), 1371–1395. doi:10.1080/01431160903548013

Gafurov, A., and Bárdossy, A. (2009). Cloud removal methodology from MODIS snow cover product. *Hydrol. Earth Syst. Sci.* 13 (7), 1361–1373. doi:10.5194/hess-13-1361-2009

Gafurov, A., Vorogushyn, S., Farinotti, D., Duethmann, D., Merkushkin, A., and Merz, B. (2015). Snow-cover reconstruction methodology for mountainous regions based on historic *in situ* observations and recent remote sensing data. *Cryosphere* 9 (2), 451–463. doi:10.5194/tc-9-451-2015

Gafurov, A., Lüdtke, S., Unger-Shayesteh, K., Vorogushyn, S., Schöne, T., Schmidt, S., et al. (2016). MODSNOW-Tool: an operational tool for daily snow cover monitoring using MODIS data. *Environ. Earth Sci.* 75 (14), 1078. doi:10.1007/s12665-016-5869-x

Gao, Y., Xie, H., Lu, N., Yao, T., and Liang, T. (2010a). Toward advanced daily cloud-free snow cover and snow water equivalent products from Terra–Aqua MODIS and Aqua AMSR-E measurements. *J. Hydrology* 385 (1), 23–35. doi:10.1016/j.jhydrol.2010.01.022

Gao, Y., Xie, H., Yao, T., and Xue, C. (2010b). Integrated assessment on multitemporal and multi-sensor combinations for reducing cloud obscuration of MODIS snow cover products of the Pacific Northwest USA. *Remote Sens. Environ.* 114 (8), 1662–1675. doi:10.1016/j.rse.2010.02.017

Gao, M., Gu, X., Liu, Y., Zhan, Y., Wei, X., Yu, H., et al. (2022). An improved spatiotemporal data fusion method for snow-covered mountain areas using snow index and elevation information. *Sensors* 22 (21), 8524. doi:10.3390/s22218524

Gao, Y., Wang, X., Mou, N., Dai, Y., Che, T., and Yao, T. (2024a). Evaluating MODIS cloud-free snow cover datasets using massive spatial benchmark data in the Tibetan Plateau. *Sci. Total Environ.* 949, 175245. doi:10.1016/j.scitotenv. 2024.175245

Gao, Z., Liu, Z., Han, P., and Zhang, C. (2024b). Investigating spatial-temporal trend of snow cover over the three provinces of Northeast China based on a cloud-free MODIS snow cover product. *J. Hydrology* 645, 132044. doi:10.1016/j.jhydrol. 2024.132044

Gascoin, S., Hagolle, O., Huc, M., Jarlan, L., Dejoux, J. F., Szczypta, C., et al. (2015). A snow cover climatology for the Pyrenees from MODIS snow products. *Hydrol. Earth Syst. Sci.* 19 (5), 2337–2351. doi:10.5194/hess-19-2337-2015

- Gascoin, S., Grizonnet, M., Bouchet, M., Salgues, G., and Hagolle, O. (2019). Theia Snow collection: high-resolution operational snow cover maps from Sentinel-2 and Landsat-8 data. *Earth Syst. Sci. Data* 11 (2), 493–514. doi:10.5194/essd-11-493-2019
- Geer, A. J. (2021). Learning earth system models from observations: machine learning or data assimilation? *Philosophical Trans. R. Soc. A Math. Phys. Eng. Sci.* 379 (2194), 20200089. doi:10.1098/rsta.2020.0089
- Ghamisi, P., Rasti, B., Yokoya, N., Wang, Q., Hofle, B., Bruzzone, L., et al. (2019). Multisource and multitemporal data fusion in remote sensing: a comprehensive review of the state of the art. *IEEE Geoscience Remote Sens. Mag.* 7 (1), 6–39. doi:10.1109/mgrs.2018.2890023
- Girotto, M., Musselman, K. N., and Essery, R. L. H. (2020). Data assimilation improves estimates of climate-sensitive seasonal snow. *Curr. Clim. Change Rep.* 6 (3), 81–94. doi:10.1007/s40641-020-00159-7
- Grünewald, T., Bühler, Y., and Lehning, M. (2014). Elevation dependency of mountain snow depth. *Cryosphere* 8 (6), 2381–2394. doi:10.5194/tc-8-2381-2014
- Guglielmin, M., Aldighieri, B., and Testa, B. (2003). PERMACLIM: a model for the distribution of mountain permafrost, based on climatic observations. *Geomorphology* 51 (4), 245–257. doi:10.1016/s0169-555x(02)00221-0
- Guo, H., Wang, X., Shen, Y., Han, C., Li, Z., Zheng, Z., et al. (2024). Development of a cloud-free MODIS NDSI dataset (2001–2020) over Northeast China. *Int. J. Digital Earth.* 17 (1). doi:10.1080/17538947.2024.2398062
- Guo, H., Wang, X., Ouyang, Z., Chen, S., Che, T., and Zheng, Z. (2025). Application of the ESTARFM algorithm for fusing Sentinel-2 and MODIS NDSI series in the eastern Qilian Mountains. *J. Hydrology Regional Stud.* 57, 102103. doi:10.1016/j.ejrh.2024.102103
- Hall, D. K., and Riggs, G. A. (2007). Accuracy assessment of the MODIS snow products. *Hydrol. Process.* 21 (12), 1534–1547. doi:10.1002/hyp.6715
- Hall, D. K., Riggs, G. A., Salomonson, V. V., Digirolamo, N. E., and Bayr, K. J. (2002). MODIS snow-cover products. *Remote Sens. Environ.* 83 (1), 181–194. doi:10.1016/s0034-4257(02)00095-0
- Hall, D. K., Riggs, G. A., Foster, J. L., and Kumar, S. V. (2010). Development and evaluation of a cloud-gap-filled MODIS daily snow-cover product. *Remote Sens. Environ.* 114 (3), 496–503. doi:10.1016/j.rse.2009.10.007
- Hall, D. K., Riggs, G. A., Digirolamo, N. E., and Román, M. O. (2019). Evaluation of MODIS and VIIRS cloud-gap-filled snow-cover products for production of an Earth science data record. *Hydrol. Earth Syst. Sci.* 23 (12), 5227–5241. doi:10.5194/hess-23-5227-2018
- Han, L., Wu, T., Liu, Z., and Liu, Q. (2019a). Cloud detection in Landsat imagery using the fractal summation method and spatial point-pattern analysis in *Geo-informatics in Sustainable Ecosystem and Society. GSES 2018. Communications in Computer and Information Science.* Editors Y. Xie, A. Zhang, H. Liu, and L. Feng (Singapore: Springer), 980. doi:10.1007/978-981-13-7025-0\_21
- Han, P., Long, D., Han, Z., Du, M., Dai, L., and Hao, X. (2019b). Improved understanding of snowmelt runoff from the headwaters of China's Yangtze River using remotely sensed snow products and hydrological modeling. *Remote Sens. Environ.* 224, 44–59. doi:10.1016/j.rse.2019.01.041
- Hao, X., Huang, X., Zhang, Y., Tang, Z., and Li, X. (2014). "HiWATER:Dataset of fractional snow cover area in the Heihe River Basin," in *National Tibetan plateau data center*. Editor C. National Tibetan Plateau Data. doi:10.3972/hiwater.218.2014.db
- Hao, X., Luo, S., Che, T., Wang, J., Li, H., Dai, L., et al. (2019). Accuracy assessment of four cloud-free snow cover products over the Qinghai-Tibetan Plateau. *Int. J. Digital Earth* 12 (4), 375–393. doi:10.1080/17538947.2017.1421721
- Hao, X., Huang, G., Che, T., Ji, W., Sun, X., Zhao, Q., et al. (2021). The NIEER AVHRR snow cover extent product over China a long-term daily snow record for regional climate research. *Earth Syst. Sci. Data* 13 (10), 4711–4726. doi:10.5194/essd-13-4711-2021
- Hao, X., Huang, G., Zheng, Z., Sun, X., Ji, W., Zhao, H., et al. (2022). Development and validation of a new MODIS snow-cover-extent product over China. *Hydrol. Earth Syst. Sci.* 26 (8), 1937–1952. doi:10.5194/hess-26-1937-2022
- Hao, X., Dai, L., and Che, T. (2025). "A dataset of 5km snow cover area on the Qinghai Tibet Plateau (1980-2020)," in *National Tibetan plateau data center*. Editor C. National Tibetan Plateau Data doi:10.11888/Cryos.tpdc.302491
- Haseeb Azizi, A., Akhtar, F., Kusche, J., Tischbein, B., Borgemeister, C., and Agumba Oluoch, W. (2024). Machine learning-based estimation of fractional snow cover in the Hindukush Mountains using MODIS and Landsat data. *J. Hydrology* 638, 131579. doi:10.1016/j.jhydrol.2024.131579
- Helmert, J., Şensoy Şorman, A., Alvarado Montero, R., De Michele, C., De Rosnay, P., Dumont, M., et al. (2018). Review of snow data assimilation methods for hydrological, land surface, meteorological and climate models: results from a COST HarmoSnow survey. *Geosciences* 8, 489. doi:10.3390/geosciences8120489
- Hoppinen, Z., Palomaki, R. T., Brencher, G., Dunmire, D., Gagliano, E., Marziliano, A., et al. (2024). Evaluating snow depth retrievals from Sentinel-1 volume scattering over NASA SnowEx sites. *Cryosphere* 18 (11), 5407–5430. doi:10.5194/tc-18-5407-2024
- Hori, M., Sugiura, K., Kobayashi, K., Aoki, T., Tanikawa, T., Kuchiki, K., et al. (2017). A 38-year (1978–2015) Northern Hemisphere daily snow cover extent product derived

- using consistent objective criteria from satellite-borne optical sensors. *Remote Sens. Environ.* 191, 402–418. doi:10.1016/j.rse.2017.01.023
- Hou, J., and Huang, C. (2016). Cloud removal for MODIS Fractional Snow Cover products by similar pixel replacement guild with modified non-dominated sorting genetic algorithm (Beijing, China: IEEE International Geoscience and Remote Sensing Symposium (IGARSS)), 4913–4916. doi:10.1109/IGARSS.2016. 7730282
- Hou, X., Zheng, Z., Li, S., Chen, X., and Cui, Y. (2018). Generation of daily cloudless snow cover product in the past 15 years in Xinjiang and accuracy validation. *Remote Sens. Land and Resour.* 30 (2), 214–222. doi:10.6046/gtzyyg.2018.02.29
- Hou, J., Huang, C., Zhang, Y., Guo, J., and Gu, J. (2019). Gap-filling of MODIS fractional snow cover products via non-local spatio-temporal filtering based on machine learning techniques. *Remote Sens. (Basel)*. 11 (1), 90. doi:10.3390/rs1101090
- Hou, J., Huang, C., Zhang, Y., and You, Y. (2022). Reconstructing a gap-free MODIS normalized difference snow index product using a long short-term memory network. *IEEE Trans. Geoscience Remote Sens.* 60, 1–14. doi:10.1109/tgrs.2022.3178421
- Hua, X., Bian, J., and Yin, G. (2025). Satellite-based assessment of snow dynamics and climatic drivers in the changbai mountain region (2001–2022). Remote Sens. (Basel). 17, 442. doi:10.3390/rs17030442
- Huang, Y., and Xu, J. (2022). HMRFS-TP: long-term daily gap-free snow cover products over the Tibetan Plateau (2002–2024). *Natl. Tibet. Plateau/Third Pole Environ. Data Cent.* doi:10.11888/Cryos.tpdc.272204
- Huang, X., Hao, X., Feng, Q., Wang, W., and Liang, T. (2014). A new MODIS daily cloud free snow cover mapping algorithm on the Tibetan Plateau. *Sci. Cold Arid Regions* 6 (2), 116–123. doi:10.3724/SPJ.1226.2014.00116
- Huang, X., Deng, J., Ma, X., Wang, Y., Feng, Q., Hao, X., et al. (2016). Spatiotemporal dynamics of snow cover based on multi-source remote sensing data in China. *Cryosphere* 10 (5), 2453–2463. doi:10.5194/tc-10-2453-2016
- Huang, Y., Liu, H., Yu, B., Wu, J., Kang, E. L., Xu, M., et al. (2018). Improving MODIS snow products with a HMRF-based spatio-temporal modeling technique in the Upper Rio Grande Basin. *Remote Sens. Environ.* 204, 568–582. doi:10.1016/j.rse.2017. 10.001
- Huang, Y., Song, Z., Yang, H., Yu, B., Liu, H., Che, T., et al. (2022a). Snow cover detection in mid-latitude mountainous and polar regions using nighttime light data. *Remote Sens. Environ.* 268, 112766. doi:10.1016/j.rse.2021.112766
- Huang, Y., Xu, J., Xu, J., Zhao, Y., Yu, B., Liu, H., et al. (2022b). HMRFS-TP: long-term daily gap-free snow cover products over the Tibetan Plateau from 2002 to 2021 based on hidden Markov random field model. *Earth Syst. Sci. Data* 14 (9), 4445–4462. doi:10.5194/essd-14-4445-2022
- Huang, J., Jiang, L., Pan, F., Zhong, B., Wu, S., and Cui, H. (2025). Estimation and evaluation of the FY-3D/MERSI-II fractional snow cover in China. *IEEE J. Sel. Top. Appl. Earth Observations Remote Sens.* 18, 2497–2511. doi:10.1109/jstars.2024.3517845
- Hüsler, F., Jonas, T., Riffler, M., Musial, J. P., and Wunderle, S. (2014). A satellite-based snow cover climatology (1985–2011) for the European Alps derived from AVHRR data. *Cryosphere* 8 (1), 73–90. doi:10.5194/tc-8-73-2014
- Jain, S. K., Goswami, A., and Saraf, A. K. (2009). Role of elevation and aspect in snow distribution in western himalaya. *Water Resour. Manag.* 23 (1), 71–83. doi:10.1007/s11269-008-9265-5
- Jing, Y., Shen, H., Li, X., and Guan, X. (2019). A two-stage fusion framework to generate a spatio–temporally continuous MODIS NDSI product over the Tibetan plateau. *Remote Sens. (Basel).* 11, 2261. doi:10.3390/rs11192261
- Jing, Y., Li, X., and Shen, H. (2022). STAR NDSI collection: a cloud-free MODIS NDSI dataset (2001–2020) for China. *Earth Syst. Sci. Data* 14 (7), 3137–3156. doi:10.5194/essd-14-3137-2022
- John, A., Cannistra, A. F., Yang, K., Tan, A., Shean, D., Hille Ris Lambers, J., et al. (2022). High-resolution snow-covered area mapping in forested mountain ecosystems using PlanetScope imagery. *Remote Sens.* 14 (14), 3409. doi:10.3390/rs14143409
- Kato, S., Loeb, N. G., Minnis, P., Francis, J. A., Charlock, T. P., Rutan, D. A., et al. (2006). Seasonal and interannual variations of top-of-atmosphere irradiance and cloud cover over polar regions derived from the CERES data set. *Geophys. Res. Lett.* 33 (19). doi:10.1029/2006gl026685
- Koehler, J., Bauer, A., Dietz, A. J., and Kuenzer, C. (2022). Towards forecasting future snow cover dynamics in the European alps—the potential of long optical remotesensing time series. *Sens. Time Ser.* 14 (18), 4461. doi:10.3390/rs14184461
- Kollert, A., Mayr, A., Dullinger, S., Hülber, K., Moser, D., Lhermitte, S., et al. (2024). Downscaling MODIS NDSI to Sentinel-2 fractional snow cover by random forest regression. *Remote Sens. Lett.* 15 (4), 363–372. doi:10.1080/2150704x.2024.2327084
- Kulkarni, A. V., Srinivasulu, J., Manjul, S. S., and P, M. (2002). Field based spectral reflectance studies to develop NDSI method for snow cover monitoring. *J. Indian Soc. Remote Sens.* 30 (1), 73–80. doi:10.1007/bf02989978
- Li, C., Su, F., Yang, D., Tong, K., Meng, F., and Kan, B. (2018). Spatiotemporal variation of snow cover over the Tibetan Plateau based on MODIS snow product, 2001–2014. *Int. J. Climatol.* 38 (2), 708–728. doi:10.1002/joc.5204

- Li, X., Jing, Y., Shen, H., and Zhang, L. (2019a). The recent developments in cloud removal approaches of MODIS snow cover product. *Hydrol. Earth Syst. Sci.* 23 (5), 2401–2416. doi:10.5194/hess-23-2401-2019
- Li, Y., Chen, Y., and Li, Z. (2019b). Developing daily cloud-free snow composite products from MODIS and IMS for the tienshan mountains. *Earth Space Sci.* 6 (2), 266–275. doi:10.1029/2018ea000460
- Li, L., Zhang, J., Sun, Z., Liu, Q., Bai, Y., Zhang, S., et al. (2022). Spatiotemporal dynamics of snow cover in typical regions of China based on FY-3 meteorological satellite. *Trans. Atmos. Sci.* 45 (06), 879–889. doi:10.13878/j.cnki.dqkxxb.20211228001
- Li, M., Zhu, X., Li, N., and Pan, Y. (2020). Gap-filling of a MODIS normalized difference snow index product based on the similar pixel selecting algorithm: a case study on the Qinghai–Tibetan Plateau. *Remote sens.* 12 (7), 1077. doi:10.3390/rs12071077
- Liang, T., Zhang, X., Xie, H., Wu, C., Feng, Q., Huang, X., et al. (2008a). Toward improved daily snow cover mapping with advanced combination of MODIS and AMSR-E measurements. *Remote Sens. Environ.* 112 (10), 3750–3761. doi:10.1016/j.rse.2008.05.010
- Liang, T. G., Huang, X. D., Wu, C. X., Liu, X. Y., Li, W. L., Guo, Z. G., et al. (2008b). An application of MODIS data to snow cover monitoring in a pastoral area: a case study in Northern Xinjiang, China. *Remote Sens. Environ.* 112 (4), 1514–1526. doi:10.1016/j.rse.2007.06.001
- Lievens, H., Brangers, I., Marshall, H. P., Jonas, T., Olefs, M., and De Lannoy, G. (2022). Sentinel-1 snow depth retrieval at sub-kilometer resolution over the European Alps. *Cryosphere* 16 (1), 159–177. doi:10.5194/tc-16-159-2022
- Lindsay, C., Zhu, J., Miller, A. E., Kirchner, P., and Wilson, T. L. (2015). Deriving snow cover metrics for alaska from MODIS. *Remote Sens.* 7 (10), 12961–12985. doi:10.3390/rs71012961
- Liu, C., Li, Z., Zhang, P., Zeng, J., Gao, S., and Zheng, Z. (2020). An assessment and error analysis of MOD10A1 snow product using Landsat and ground observations over China during 2000–2016. *IEEE J. Sel. Top. Appl. Earth Observations Remote Sens.* 13, 1467–1478. doi:10.1109/jstars.2020.2983550
- Liu, Y., Fang, Y., and Margulis, S. A. (2021). Spatiotemporal distribution of seasonal snow water equivalent in High Mountain Asia from an 18-year Landsat–MODIS era snow reanalysis dataset. *Cryosphere* 15 (11), 5261–5280. doi:10.5194/tc-15-5261-2021
- Liu, A., Che, T., Huang, X., Dai, L., Wang, J., and Deng, J. (2022a). Effect of cloud mask on the consistency of snow cover products from MODIS and VIIRS. Remote sens. 14 (23), 6134. doi:10.3390/rs14236134
- Liu, Y., Fang, Y., Li, D., and Margulis, S. A. (2022b). How well do global snow products characterize snow storage in High Mountain Asia? *Geophys. Res. Lett.* 49 (16), e2022GL100082. doi:10.1029/2022gl100082
- Liu, D., Shen, Y., Wang, Y., Wang, Z., Mo, Z., and Zhang, Q. (2023). Monitoring the spatiotemporal dynamics of arctic winter snow/ice with moonlight remote sensing: systematic evaluation in svalbard. *Remote Sens. (Basel).* 15, 1255. doi:10.3390/rs15051255
- López-Burgos, V., Gupta, H. V., and Clark, M. (2013). Reducing cloud obscuration of MODIS snow cover area products by combining spatio-temporal techniques with a probability of snow approach. *Hydrol. Earth Syst. Sci.* 17 (5), 1809–1823. doi:10.5194/hess-17-1809-2013
- Lv, Z., Pomeroy, J. W., and Fang, X. (2019). Evaluation of SNODAS snow water equivalent in western Canada and assimilation into a Cold region hydrological model. *Water Resour. Res.* 55 (12), 11166–11187. doi:10.1029/2019wr025333
- Mao, K., Yuan, Z., Zuo, Z., Xu, T., Shen, X., and Gao, C. (2019). Changes in global cloud cover based on remote sensing data from 2003 to 2012. *Chin. Geogr. Sci.* 29 (2), 306–315. doi:10.1007/s11769-019-1030-6
- Margulis, S. A., Liu, Y., and Baldo, E. (2019). A joint Landsat- and MODIS-based reanalysis approach for midlatitude montane seasonal snow characterization. *Front. Earth Sci.* 7, 272–6463. doi:10.3389/feart.2019.00272
- Mattar, C., Fuster, R., and Perez, T. (2022). Application of a cloud removal algorithm for snow-covered areas from daily MODIS imagery over andes mountains. *Atmos.* (*Basel*). 13, 392. doi:10.3390/atmos13030392
- Min, W., Pen, J., and Li, S. (2021). The evaluation of FY-3C snow products in the Tibetan Plateau. Remote Sens. Land and Resour. 33 (01), 145-151. doi:10.6046/gtzyyg.2020102
- Mishra, P., Zaphu, V. V., Monica, N., Bhadra, A., and Bandyopadhyay, A. (2016). Accuracy assessment of MODIS fractional snow cover product for eastern himalayan catchment. *J. Indian Soc. Remote Sens.* 44 (6), 977–985. doi:10.1007/s12524-016-0548-7
- Molotch, N. P., and Margulis, S. A. (2008). Estimating the distribution of snow water equivalent using remotely sensed snow cover data and a spatially distributed snowmelt model: a multi-resolution, multi-sensor comparison. *Adv. Water Resour.* 31 (11), 1503–1514. doi:10.1016/j.advwatres.2008.07.017
- Muhuri, A., Gascoin, S., Menzel, L., Kostadinov, T. S., Harpold, A. A., Sanmiguel-Vallelado, A., et al. (2021). Performance assessment of optical satellite-based operational snow cover monitoring algorithms in forested landscapes. *IEEE J. Sel. Top. Appl. Earth Observations Remote Sens.* 14, 7159–7178. doi:10.1109/jstars.2021.3089655

- Musselman, K. N., Addor, N., Vano, J. A., and Molotch, N. P. (2021). Winter melt trends portend widespread declines in snow water resources. *Nat. Clim. Change* 11 (5), 418–424. doi:10.1038/s41558-021-01014-9
- Newfel, M., Ahmet, E. T., Hongjie, X., Hatim, I. S., and Almoutaz, A. E. H. (2013). Assessment of ice mapping system and moderate resolution imaging spectroradiometer snow cover maps over Colorado Plateau. *J. Appl. Remote Sens.* 7 (1), 073540. doi:10.1117/1.jrs.7.073540
- Pan, F., Jiang, L., Wang, G., Pan, J., Huang, J., Zhang, C., et al. (2024). MODIS daily cloud-gap-filled fractional snow cover dataset of the Asian Water Tower region (2000–2022). *Earth Syst. Sci. Data* 16 (5), 2501–2523. doi:10.5194/essd-16-2501-2024
- Pandya, D., Vachharajani, B., and Srivastava, R. (2022). A review of data assimilation techniques: applications in engineering and agriculture. *Mater. Today Proc.* 62, 7048–7052. doi:10.1016/j.matpr.2022.01.122
- Parajka, J., and Blöschl, G. (2008). Spatio-temporal combination of MODIS images potential for snow cover mapping. *Water Resour. Res.* 44 (3). doi:10.1029/2007wr006204
- Parajka, J., Pepe, M., Rampini, A., Rossi, S., and Blöschl, G. (2010). A regional snow-line method for estimating snow cover from MODIS during cloud cover. *J. Hydrology* 381 (3), 203–212. doi:10.1016/j.jhydrol.2009.11.042
- Parajka, J., Holko, L., Kostka, Z., and Blöschl, G. (2012). MODIS snow cover mapping accuracy in a small mountain catchment comparison between open and forest sites. *Hydrol. Earth Syst. Sci.* 16 (7), 2365–2377. doi:10.5194/hess-16-2365-2012
- Paudel, K. P., and Andersen, P. (2011). Monitoring snow cover variability in an agropastoral area in the Trans Himalayan region of Nepal using MODIS data with improved cloud removal methodology. *Remote Sens. Environ.* 115 (5), 1234–1246. doi:10.1016/j.rse.2011.01.006
- Poussin, C., Peduzzi, P., Chatenoux, B., and Giuliani, G. (2025). A 37 years [1984–2021] Landsat/Sentinel-2 derived snow cover time-series for Switzerland. *Sci. Data* 12 (1), 632. doi:10.1038/s41597-025-04961-6
- Qin, Y., Abatzoglou, J. T., Siebert, S., Huning, L. S., Aghakouchak, A., Mankin, J. S., et al. (2020). Agricultural risks from changing snowmelt. *Nat. Clim. Change* 10 (5), 459–465. doi:10.1038/s41558-020-0746-8
- Qiu, Y., and Wang, X. (2021). Daily fractional snow cover dataset over High Asia during 2002 to 2018. National Cryosphere Desert Data Center. doi:10.11922/sciencedb.457
- Qiu, Y., Zhang, H., Chu, D., Zhang, X., Yu, X., and Zheng, Z. (2017). Cloud removing algorithm for the daily cloud free MODIS-based snow cover product over the Tibetan Plateau. *J. Glaciol. Geocryol.* 39 (03), 515–526. doi:10.7522/j.issn.1000-0240.2017.0058
- Revuelto, J., Alonso-González, E., Gascoin, S., Rodríguez-López, G., and López-Moreno, J. I. (2021). Spatial downscaling of MODIS snow cover observations using sentinel-2 snow products. *Remote Sens.* 13 (22): 4513. doi:10.3390/rs13224513
- Richiardi, C., Blonda, P., Rana, F. M., Santoro, M., Tarantino, C., Vicario, S., et al. (2021). A revised snow cover algorithm to improve discrimination between snow and clouds: a case study in gran paradiso national Park. *Remote Sens. (Basel)*. 13, 1957. doi:10.3390/rs13101957
- Richiardi, C., Siniscalco, C., and Adamo, M. (2023). Comparison of three different random forest approaches to retrieve daily high-resolution snow cover maps from MODIS and sentinel-2 in a mountain area, gran paradiso national park (NW alps). *Remote Sens.* 15 (2), 343. doi:10.3390/rs15020343
- Riggs, G., and Hall, D. (2010). MODIS snow and ice products, and their assessment and applications. in *Land Remote Sensing and Global Environmental Change. Remote Sensing and Digital Image Processing.* Editors B. Ramachandran, C. Justice, and M. Abrams. (New York, NY: Springer) 12. doi:10.1007/978-1-4419-6749-7\_30
- Riggs, G., and Hall, D. (2020). Continuity of MODIS and VIIRS snow cover extent data products for development of an Earth science data record. *Remote Sens.* 12 (22), 3781. doi:10.3390/rs12223781
- Riggs, G. A., Hall, D. K., and Román, M. O. (2017). Overview of NASA's MODIS and visible infrared imaging radiometer suite (VIIRS) snow-cover earth system data Records. *Earth Syst. Sci. Data* 9 (2), 765–777. doi:10.5194/essd-9-765-2017
- Rittger, K., Painter, T. H., and Dozier, J. (2013). Assessment of methods for mapping snow cover from MODIS. *Adv. Water Resour.* 51, 367–380. doi:10.1016/j.advwatres.2012.03.002
- Rittger, K., Bair, E. H., Kahl, A., and Dozier, J. (2016). Spatial estimates of snow water equivalent from reconstruction. *Adv. Water Resour.* 94, 345–363. doi:10.1016/j.advwatres.2016.05.015
- Rittger, K., Krock, M., Kleiber, W., Bair, E. H., Brodzik, M. J., Stephenson, T. R., et al. (2021). Multi-sensor fusion using random forests for daily fractional snow cover at 30 m. *Remote Sens. Environ.* 264, 112608. doi:10.1016/j.rse.2021.112608
- Román, M. O., Justice, C., Paynter, I., Boucher, P. B., Devadiga, S., Endsley, A., et al. (2024). Continuity between NASA MODIS collection 6.1 and VIIRS collection 2 land products. *Remote Sens. Environ.* 302, 113963. doi:10.1016/j.rse.2023. 113963
- Romanov, P. (2017). Global multisensor automated satellite-based snow and ice mapping system (GMASI) for cryosphere monitoring. *Remote Sens. Environ.* 196, 42–55. doi:10.1016/j.rse.2017.04.023

- Romanov, P., Gutman, G., and Csiszar, I. (2000). Automated monitoring of snow cover over North America with Multispectral satellite data. *J. Appl. Meteorology* 39 (11), 1866–1880. doi:10.1175/1520-0450(2000)039<1866:amosco>2.0.co;2
- Salomonson, V. V., and Appel, I. (2004). Estimating fractional snow cover from MODIS using the normalized difference snow index. *Remote Sens. Environ.* 89 (3), 351–360. doi:10.1016/j.rse.2003.10.016
- Samadzadegan, F., Toosi, A., and Dadrass Javan, F. (2025). A critical review on multisensor and multi-platform remote sensing data fusion approaches: current status and prospects. *Int. J. Remote Sens.* 46 (3), 1327–1402. doi:10.1080/01431161.2024.2429784
- Singh, M. K., Thayyen, R. J., and Jain, S. K. (2021). Snow cover change assessment in the upper Bhagirathi basin using an enhanced cloud removal algorithm. *Geocarto Int.* 36 (20), 2279–2302. doi:10.1080/10106049.2019.1704069
- Stillinger, T., Rittger, K., Raleigh, M. S., Michell, A., Davis, R. E., and Bair, E. H. (2023). Landsat, MODIS, and VIIRS snow cover mapping algorithm performance as validated by airborne lidar datasets. *Cryosphere* 17 (2), 567–590. doi:10.5194/tc-17-567-2023
- Tang, Z., Wang, J., Li, H., and Yan, L. (2013). Spatiotemporal changes of snow cover over the Tibetan plateau based on cloud-removed moderate resolution imaging spectroradiometer fractional snow cover product from 2001 to 2011. *J. Appl. Remote Sens.* 7, 073582. doi:10.1117/1.jrs.7.073582
- Thackeray, C. W., Derksen, C., Fletcher, C. G., and Hall, A. (2019). Snow and climate: feedbacks, Drivers, and Indices of change. *Curr. Clim. Change Rep.* 5 (4), 322–333. doi:10.1007/s40641-019-00143-w
- Thiebault, K., and Young, S. (2020). Snow cover change and its relationship with land surface temperature and vegetation in northeastern North America from 2000 to 2017. *Int. J. Remote Sens.* 41 (21), 8453–8474. doi:10.1080/01431161.2020.1779379
- Tong, J., Déry, S. J., and Jackson, P. L. (2009). Interrelationships between MODIS/Terra remotely sensed snow cover and the hydrometeorology of the Quesnel River Basin, British Columbia, Canada. *Hydrol. Earth Syst. Sci.* 13 (8), 1439–1452. doi:10.5194/hess-13-1439-2009
- Vuyovich, C. M., Jacobs, J. M., and Daly, S. F. (2014). Comparison of passive microwave and modeled estimates of total watershed SWE in the continental United States. *Water Resour. Res.* 50 (11), 9088–9102. doi:10.1002/2013wr014734
- Wang, J. (2022). Preparation of AVHRR snow cover extent dataset in the Northern Hemisphere and characteristics of snow phenology. (master's thesis). Taiyuan University of Technology. doi:10.27352/d.cnki.gylgu.2022.000607
- Wang, X., Xie, H., and Liang, T. (2008). Evaluation of MODIS snow cover and cloud mask and its application in Northern Xinjiang, China. *Remote Sens. Environ.* 112 (4), 1497–1513. doi:10.1016/j.rse.2007.05.016
- Wang, J., Hao, X., He, D., Wang, J., Li, H., and Zhao, Q. (2022a). Snow discrimination algorithm in the Northern Hemisphere based on AVHRR image. *J. Glaciol. Geocryol.* 44 (1), 316–326. doi:10.7522/j.issn.1000-0240.2022.0039
- Wang, Y., Gu, L., Li, X., Gao, F., Jiang, T., and Ren, R. (2022b). An improved spatiotemporal fusion algorithm for monitoring daily snow cover changes with high spatial resolution. *IEEE Trans. Geoscience Remote Sens.* 60, 1–17. doi:10.1109/tgrs.2022.3224126
- Wang, Y., Su, J., Zhai, X., Meng, F., and Liu, C. (2022c). Snow coverage mapping by learning from sentinel-2 satellite multispectral images via machine learning algorithms. *Remote Sens.* 14 (3), 782. doi:10.3390/rs14030782
- Wang, Z., Fan, B., Tu, Z., Li, H., and Chen, D. (2022d). Cloud and snow identification based on DeepLab V3+ and CRF combined model for GF-1 WFV images. *Remote Sens.* (*Basel*). 14, 4880. doi:10.3390/rs14194880
- Wang, Y., Gu, L., Li, X., Gao, F., and Jiang, T. (2023). Coexisting cloud and snow detection based on a hybrid features network applied to remote sensing images. *IEEE Trans. Geoscience Remote Sens.* 61, 1–15. doi:10.1109/tgrs.2023.3299617
- Wang, J., Li, B., Li, Y., Lian, L., Dong, F., Zhu, Y., et al. (2025a). A daily snow cover dataset for central eurasia during autumn from 2004 to 2021. *Geoscience Data J.* 12 (3), e70017. doi:10.1002/gdj3.70017
- Wang, Q., Ma, Y., Xu, Z., and Li, J. (2025b). Accuracy assessment of cloud removal methods for Moderate-resolution Imaging Spectroradiometer (MODIS) snow data in the Tianshan Mountains, China. *J. Arid Land* 17 (4), 457–480. doi:10.1007/s40333-025-0098-3
- Warren, S. G. (1982). Optical properties of snow. Rev. Geophys. 20 (1), 67-89. doi:10.1029/rg020i001p00067
- Warren, S. G. (2019). Optical properties of ice and snow. *Philosophical Trans. R. Soc. A Math. Phys. Eng. Sci.* 377 (2146), 20180161. doi:10.1098/rsta.2018.0161
- Wu, T., Han, L., and Liu, Q. (2019). A novel algorithm for differentiating cloud from snow sheets using Landsat 8 OLI imagery. *Adv. Space Res.* 64 (1), 79–87. doi:10.1016/j.asr.2019.03.014
- Wu, X., Naegeli, K., Premier, V., Marin, C., Ma, D., Wang, J., et al. (2021). Evaluation of snow extent time series derived from Advanced Very High Resolution Radiometer global area coverage data (1982–2018) in the Hindu Kush Himalayas. *Cryosphere* 15 (9), 4261–4279. doi:10.5194/tc-15-4261-2021
- Xiao, X., Liang, S., He, T., Wu, D., Pei, C., and Gong, J. (2021). Estimating fractional snow cover from passive microwave brightness temperature data using MODIS snow

- cover product over North America. Cryosphere~15~(2), 835-861.~doi:10.5194/tc-15-835-2021
- Xiao, X., He, T., Liang, S., Liang, S., Liu, X., Ma, Y., et al. (2024). Towards a gapless 1 km fractional snow cover via a data fusion framework. *ISPRS J. Photogrammetry Remote Sens.* 215, 419–441. doi:10.1016/j.isprsjprs.2024.07.018
- Xing, D., Hou, J., Huang, C., and Zhang, W. (2022). Spatiotemporal reconstruction of MODIS normalized difference snow index products using U-net with partial convolutions. *Remote Sens.* (*Basel*). 14, 1795. doi:10.3390/rs14081795
- Xu, J., Hua, R., Wang, S., Lhermitte, S., Gu, Q., Yu, B., et al. (2025). MAT-MS: a mask-aware transformer for constructing gap-free MODIS normalized difference snow index products. *ISPRS J. Photogrammetry Remote Sens.* 227, 775–788. doi:10.1016/j.isprsjprs.2025.07.004
- Yan, D., Zhang, Y., and Gao, H. (2024). Development of a daily cloud-free snow-cover dataset using MODIS-based snow-cover probability for High Mountain Asia during 2000–2020. *Remote Sens. (Basel)*. 16, 2956. doi:10.3390/rs16162956
- Yang, Y., Chen, R., Liu, G., Liu, Z., and Wang, X. (2022). Trends and variability in snowmelt in China under climate change. *Hydrol. Earth Syst. Sci.* 26 (2), 305–329. doi:10.5194/hess-26-305-2022
- Yang, K., John, A., Shean, D., Lundquist, J. D., Sun, Z., Yao, F., et al. (2023). High-resolution mapping of snow cover in montane meadows and forests using Planet imagery and machine learning. *Front. Water* 5, 1128758. doi:10.3389/frwa.2023.1128758
- Yang, J., Jiang, Y., Song, Q., Wang, Z., Hu, Y., Li, K., et al. (2025). An approach for multi-source land use and land cover data fusion considering spatial correlations. *Remote Sens. (Basel)*. 17, 1131. doi:10.3390/rs17071131
- Yang, Q., Song, K., Hao, X., Chen, S., and Zhu, B. (2018). An assessment of snow cover duration variability among three basins of songhua river in northeast China using binary decision tree. *Chin. Geogr. Sci.* 28 (6), 946–956. doi:10.1007/s11769-018-1004-0
- Yang, Y.-J., Wu, B.-D., Shi, C.-E., Zhang, J.-H., Li, Y.-B., et al. (2013). Impacts of Urbanization and Station-relocation on Surface Air Temperature Series in Anhui Province, China. *Pure Appl. Geophys.* 170 (11), 1069–1083. doi:10.1007/s00024-012-0619-9
- Yatheendradas, S., and Kumar, S. (2022). A novel machine learning-based gapfilling of fine-resolution remotely sensed snow cover fraction data by combining downscaling and regression. *J. Hydrometeorol.* 23 (5), 637–658. doi:10.1175/jhm-d-20-
- Ye, F., Cheng, Q., Hao, W., and Yu, D. (2024). Reconstructing MODIS normalized difference snow index product on Greenland ice sheet using spatiotemporal extreme gradient boosting model. *J. Hydrology* 645, 132277. doi:10.1016/j.jhydrol. 2024.132277
- Ying, J. J., Yang, J. W., Jiang, L. M., Pan, J. M., Zhang, C., Xiong, C., et al. (2025). Evaluation of the sentinel-1 SAR-based snow depth product over the northern Hemisphere. *J. Hydrology* 661, 133593. doi:10.1016/j.jhydrol.2025.133593
- You, Q., Wu, T., Shen, L., Pepin, N., Zhang, L., Jiang, Z., et al. (2020). Review of snow cover variation over the Tibetan Plateau and its influence on the broad climate system. *Earth-Science Rev.* 201, 103043. doi:10.1016/j.earscirev.2019.103043
- Yu, X. (2017). Cloud removing method and accuracy verification of snow extent product in high Asia area. (master's thesis). Liaoning Technical University. Available online at:  $https://kns.cnki.net/kcms2/article/abstract?v=ZscdH8NaPi_n4]TukE5BLV0 sbGLjkNYm7_iHzHtTZ4s2J6MsHEKvx8Uq-GeqUtUBYSm_rPBjnco_fZdpzsnvr7rsKJog21M6LsqwldXIawH4wkXtsxCm64P7UcIUH78e8Msk9rYElB bJV3jt3tiAuniTRwUj80cQLIAunlnS1Bic_w70unSm_g==&uniplatform=NZKPT&language=CHS.$
- Zakeri, F., and Mariethoz, G. (2024). Synthesizing long-term satellite imagery consistent with climate data: application to daily snow cover. *Remote Sens. Environ.* 300, 113877. doi:10.1016/j.rse.2023.113877
- Zhang, T. (2005). Influence of the seasonal snow cover on the ground thermal regime: an overview. Rev. Geophys. 43 (4). doi:10.1029/2004rg000157
- Zhang, Y.-F., and Yang, Z.-L. (2016). Estimating uncertainties in the newly developed multi-source land snow data assimilation system. *J. Geophys. Res. Atmos.* 121 (14), 8254–8268. doi:10.1002/2015jd024248
- Zhang, G., Xie, H., Yao, T., Liang, T., and Kang, S. (2012). Snow cover dynamics of four lake basins over Tibetan Plateau using time series MODIS data (2001–2010). *Water Resour. Res.* 48 (10). doi:10.1029/2012wr011971
- Zhang, H., Zhang, F., Che, T., and Wang, S. (2020a). Comparative evaluation of VIIRS daily snow cover product with MODIS for snow detection in China based on ground observations. *Sci. Total Environ.* 724, 138156. doi:10.1016/j.scitotenv.2020. 138156.
- Zhang, Y., Qin, X., Li, X., Zhao, J., and Liu, Y. (2020b). Estimation of shortwave solar radiation on clear-sky days for a valley glacier with sentinel-2 time series. *Remote Sens.* (*Basel*). 12, 927. doi:10.3390/rs12060927
- Zhang, Y., Song, Y., Ye, C., and Liu, J. (2023). An integrated approach to reconstructing snow cover under clouds and cloud shadows on Sentinel-2 Time-Series images in a mountainous area. *J. Hydrology* 619, 129264. doi:10.1016/j.jhydrol.2023.129264

Zhang, Y., Ning, G., Chen, S., and Yang, Y. (2021). Impact of rapid urban sprawl on the local meteorological observational environment based on remote sensing images and GIS technology. doi:10.3390/rs13132624

Zhang, Y., Ye, C., Yang, R., and Li, K. (2024). Reconstructing snow cover under clouds and cloud shadows by combining sentinel-2 and Landsat 8 images in a mountainous region. *Remote Sens. (Basel).* 16, 188. doi:10.3390/rs16010188

Zheng, Z., and Cao, G. (2019). Snow cover dataset based on multi-source remote sensing products blended with 1km spatial resolution on the Qinghai-Tibet Plateau (1995-2018). *Natl. Tibet. Plateau/Third Pole Environ. Data Cent.* doi:10.11888/Snow.tpdc.270102

Zhu, L. (2022). Snow-cover reconstruction at the watershed scale with fine spatial and temporal resolution based on machine learning. (doctoral dissertation). Nanjing University of Information Science and Technology. doi:10.27248/d.cnki.gnjqc.2022.000020

Zhu, X., Chen, J., Gao, F., Chen, X., and Masek, J. G. (2010). An enhanced spatial and temporal adaptive reflectance fusion model for complex heterogeneous regions. *Remote Sens. Environ.* 114 (11), 2610–2623. doi:10.1016/j.rse.2010.

Zhu, X., Helmer, E. H., Gao, F., Liu, D., Chen, J., and Lefsky, M. A. (2016). A flexible spatiotemporal method for fusing satellite images with different resolutions. *Remote Sens. Environ.* 172, 165–177. doi:10.1016/j.rse.2015.11.016

Zhu, X., Zhan, W., Zhou, J., Chen, X., Liang, Z., Xu, S., et al. (2022). A novel framework to assess all-round performances of spatiotemporal fusion models. *Remote Sens. Environ.* 274, 113002. doi:10.1016/j.rse.2022.

Zhu, L., Ma, G., Zhang, Y., Wang, J., and Kan, X. (2023). Reconstruction of snow cover in Kaidu River Basin via snow grain size gap-filling based on machine learning. Water~(Basel).~15, 3726.~doi:10.3390/w15213726